63323

AFCRL - 63 - 459

AD

AF.61(052)-400
TN-2

October, 1962

TECHNICAL NOTE NO. 2.

LUNAR INFRA-RED MEASUREMENTS

by

R. STERNBERG

Department of Astronomy,
University of Manchester.

The research reported in this document has been sponsored
by, or in part by, Cambridge Research Laboratories, OAR
through the European Office, Aerospace Research,
United States Air Force.

ABSTRACT

Following the successful development of techniques for producing multilayer interference filters for the infra-red out to 20μ, a radiometer was designed and constructed to make observations of the moon in the atmospheric window $8 - 13\mu$, using the 50-inch telescope at Asiago.

The primary aim was to use this instrument to determine the emissivity of the lunar surface by measuring the radiant flux from the moon in two or more narrow spectral regions within this band. Due to unusually unfavourable weather conditions during the first observing expedition (the only one so far) this objective could not be achieved. A number of anomalous temperature distributions were however found, which appear to be associated with ray craters.

LIST OF CONTENTS

LUNAR INFRA-RED MEASUREMENTS

INTRODUCTION

Lunar infra-red measurements were made as long ago as 1927 by Pettit and Nicholson [5]. Their results, and subsequent microwave measurements by Piddington and Minnet [6] led to the conclusion that the surface of the Moon is covered by a layer of low thermal conductivity. This material is widely assumed to be dust.

Infra-red observations during lunar eclipses by Sinton [7] and Shorthill, Borough and Colney [8] showed that certain craters cooled less rapidly than their surroundings, and in particular that Tycho was about 40 °C warmer than its surroundings about one hour after it entered the umbra. On this basis Sinton calculated that the dust thickness over Tycho was about 0.3 mm. Assuming an average meteoritic flux given by Whipple he estimates that Tycho is at the most 10^7 years old.

Isothermal contours of the entire moon at different phases were produced by Sinton [9], and of relatively small areas of the moon at higher spatial resolution by Shorthill and Saari [10]. The latter work can, however, be criticised on the grounds that the effective sensor area was larger than the spatial resolution aimed at, and that there was an uncertainty of up to 50″ of arc in the correlation of the area examined with the visual features.

It was therefore felt that a useful purpose would be served by the construction of an instrument, which, by employing modern infra-red techniques, could determine with the highest possible accuracy and spatial resolution, the temperature of selected, and definitely identified, areas of the lunar surface.

In order to obtain absolute values of the surface temperature from the measured infra-red emission, it is necessary to know the emissivity of the surface. All previous observers have assumed that the moon can be represented in the infra-red as a perfect black body, i.e. with an emissivity equal to unity. If this should not be true, the real temperature will naturally be higher than that deduced from the infra-red measurements.

A value for the emissivity can be determined from values of the infra-red emission in at least two narrow wavelength regions. If these regions are sufficiently close together it can reasonably be assumed that the emissivity does not vary to any appreciable extent over this region. In this case it is possible to determine the temperature by comparing the ratio of the two energy fluxes with that for a perfect black body, and then to deduce the temperature from a measurement of the absolute flux at one of these wavelengths.

The regions to be used for observations on the moon are obviously limited to the transparent windows of the terrestrial atmosphere. Furthermore they have to be chosen so that the infra-red energy of reflected sunlight is so small that it can be neglected, in comparison with the thermal emission of the moon. From this point of view the obvious choice is the 8 - 13μ window. This also has the advantage of being near the maximum of the Planckian distribution for the range of temperatures to be expected on the lunar surface. Transmission curves of the actual filters used in this work are shown in figs. 18 & 19.

The work reported here falls naturally into three sections:

I) Development and production of filters for the intermediate infra-red region.

II) Design and construction of an infra-red photometer suitable for attachment to a telescope.

III) Experimental results and their reduction.

I. FILTERS FOR THE INTERMEDIATE INFRA-RED REGION.

Multilayer interference filters for the visible and near infra-red [$<5\mu$] have been developed in these laboratories by Ring [1], Lissberger [2], and Beer [3].

The main problems in extending their methods to the intermediate infra-red region are to find substances transparent to the radiations in question, which at the same time lend themselves to high vacuum deposition in the relatively thick layers required, and to develop methods of controlling the thickness of the layers to the necessary close limits.

The range over which filters could be produced was limited to 5-20μ by the control monochromator available. After overcoming a number of difficulties connected with the control system the goal of 20μ was reached, and there seems to be no reason why this limit should not be extended by using the same methods.

An intrinsic disadvantage of multilayer filters is the presence of "sidebands", i.e. transmission regions relatively close to the desired passband, which have to be suppressed by means of auxiliary filters. In some cases this can be done by making use of the absorption edges of suitable substances, used either as substrates for the multilayers, or as separate filters. In the present case of the 8-13μ band, the "cut-on" of indium antimonide at 7.8μ, and the "cut-off" of barium fluoride at 13μ are very convenient for sideband elimination. If the indium antimonide has suitable anti-reflection coatings on its surfaces, a transmission of more than 80% can be realised.

The Vacuum Plant

The vacuum plant was one which had previously been used for the production of multilayers in the near infra-red, and has been described in detail by Beer [3]. It was modified in some respects to make it more suitable for the spectral region aimed at. The main modifications consisted in replacing the tungsten spiral light source for the control system, first by a molybdenum ribbon, and later by a Nernst filament; the addition of a valve of the "butterfly" type between the vacuum chamber and the diffusion pump, enabling the chamber to be isolated and roughed down from atmospheric pressure via a by-pass line, and a completely redesigned control system, which is to be described under a separate heading. Photographs of the vacuum plant are given in Figures 16 & 17.

Fig. 16. General View of Evaporation Plant.

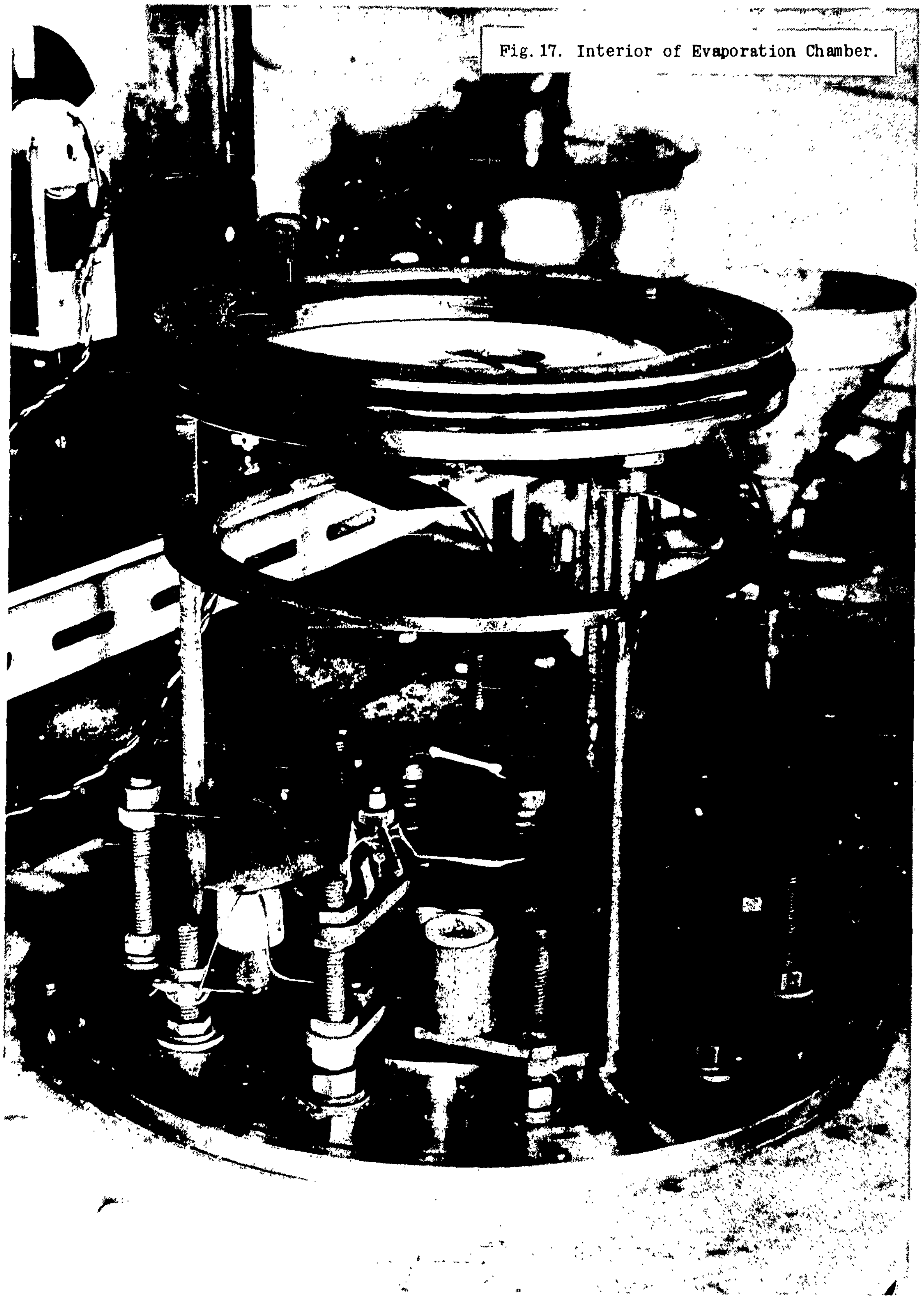

Fig. 17. Interior of Evaporation Chamber.

Substrates.

The principal requirements for substrates are:

1) Transparency in the region for which the filter is to transmit, and also preferably transparency in the visible, so that coating defects, such as pinholes, can be detected.

2) Stability on exposure to atmosphere.

3) Low refractive index, so as to minimize reflection losses on the rear surface of the filter.

4) Suitably located absorption edges, to help in eliminating side-bands.

5) Availability in sheet or film form, or with physical characteristics enabling optical surfaces to be produced by conventional means.

The most useful substrate material is KRS5 (thallium bromide-iodide). This substance is transparent from 0.5μ to 40μ. Its only drawback is the high cost (of the order of £60. for a 25 mm. disc), and for this reason it has not been used in the work reported here.

For the region 5μ to 10μ, CaF_2 makes a convenient substrate. It is completely unaffected by moisture in the atmosphere, and is readily polished by normal optical techniques. The onset of absorption at 10μ will suppress the long wave sidebands of filters beyond 8μ.

For filters up to 13μ, BaF_2 makes a convenient substrate, being also atmospherically stable, and only slightly more expensive than CaF_2

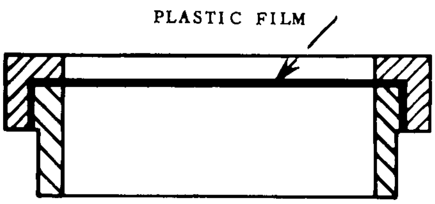

Fig. 1. Mount for Plastic Films.

From about 13μ onwards, polythene and polypropylene films make satisfactory substrates, both being free from absorption bands at least out to 25μ. Polypropylene is preferred on account of its higher melting point, resisting the heat radiated from the evaporation sources better.

The films were stretched in a metal frame, as shown in fig. 1. A second protective film could be mounted above the coated film, when hygroscopic coating materials, such as KBr, were used. Once coated, the films could not be removed from the frames without damaging the coating.

No plastic substrate material was found to cover the range from 10μ to 13μ. For filters in this region NaCl substrates could be used. In order to get good adhesion of the multilayer coatings it was found necessary to polish the plates with cerium oxide immediately prior to loading into the vacuum plant. Attempts to protect these filters from atmospheric moisture by a coating of paraffin wax were unsuccessful. If a filter in this wavelength region is required to operate exposed to a humid atmosphere it is necessary to use BaF_2 or KRS-5 substrates, or to seal the filter hermetically between cover plates of one of these materials.

Coating materials

Coating materials for multilayer filters can be divided into two groups, namely high index and low index materials. Because of the availability in the infra-red of semi-conductor materials of very high refractive index, some substances, such as ZnS, which are normally regarded as high index materials, can actually be used for low index layers. Because of multiple reflections within each layer a very small amount of absorption in the layer will reduce the filter transmission seriously. Hence the lowest possible absorption is a prime requirement for coating materials. In addition the materials should evaporate into the relatively thick films needed in the infra-red without any tendency to crack or peel off the substrate.

The high index material used throughout this work was tellurium. Other workers have used germanium for this purpose. Germanium has the disadvantage that the refractive index of the evaporated films is significantly lower than the index of the bulk material. It also is a very difficult substance to evaporate because of the high temperature required, and because of the fact that it will attack many crucible materials when molten. By contrast tellurium evaporates so readily that the main difficulty is to stop deposition when the film has reached the required thickness. The refractive index of tellurium films was found to be 4.8 to 5.0, as compared with the bulk index of 5.3 (mean of o and e indices). $\lambda/4$ films of tellurium at a wavelength of 60μ could be deposited without any difficulty.

A variety of low index materials was used, depending on the wavelength for which the filter was intended. These materials included: Cryolite, NaF, LiF, KBr, ZnS. Refractive indices and transmission limits for these materials can be found in:-

University of Michigan - Willow Run Laboratories.

State-of-the-Art Report - Optical Materials for Infra-red Instrumentation (1959).

All these materials evaporated readily to form thick films, and were compatible with the tellurium high index films. Above a certain thickness the dielectric films tended to be visually cloudy, but this did not appear to affect their infra-red performance.

Evaporation sources.

Two types of evaporation source were developed for tellurium and the dielectric materials respectively.

The tellurium source is shown diagrammatically in fig. 2. An alumina crucible is surrounded by a tungsten wire heater, and the whole is surrounded by a second larger alumina crucible serving as a heat shield. The tellurium in stick form is loaded into the inner crucible. One charge of tellurium lasts for 2-4 filters, depending on the number and thickness of the layers.

Fig. 3. shows the evaporation source for dielectrics as finally developed. A tungsten heater spiral projects through a hole in the bottom of an alumina crucible. The return lead of the heater is taken down the centre of the spiral, and insulated from it by alumina beads. The evaporant is compacted in the crucible so as to leave a hole down the centre, so that heating is by radiation only. This design gives a very rapid rate of evaporation, as it is not necessary to bring the whole charge to evaporation temperature. It also has the advantage that crucibles can be removed for recharging without disturbing the heater spiral. It was found essential that the heater projects above the top of the crucible, because otherwise a crust will form above the heater and prevent evaporation. When charging the crucible, the evaporant was made into a paste with water or, in the case of water-soluble substances, with alcohol, pressed into shape in the crucible, and baked in a furnace at approx. 200°C for 2 hours. When first heated under vacuum it was found that most dielectrics outgassed strongly, and it was necessary to bring the sources up to evaporation temperature very slowly.

A shutter, pivoted above the evaporation sources, could be operated by means of a permanent magnet from outside the vacuum chamber to terminate the evaporation when the layers had reached the desired thickness. This was quite effective with dielectric materials, but

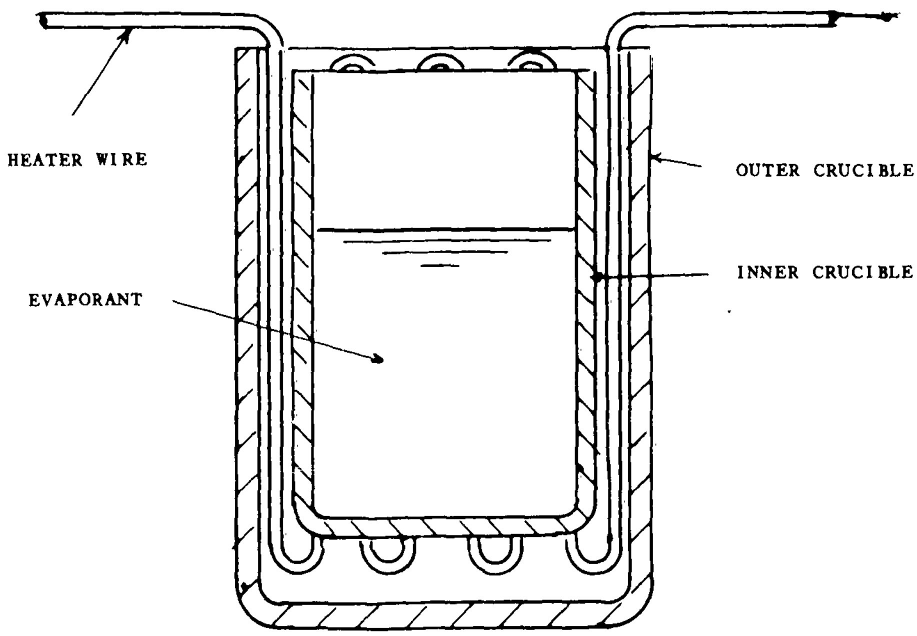

Fig. 2. Evaporation Source for Tellurium.

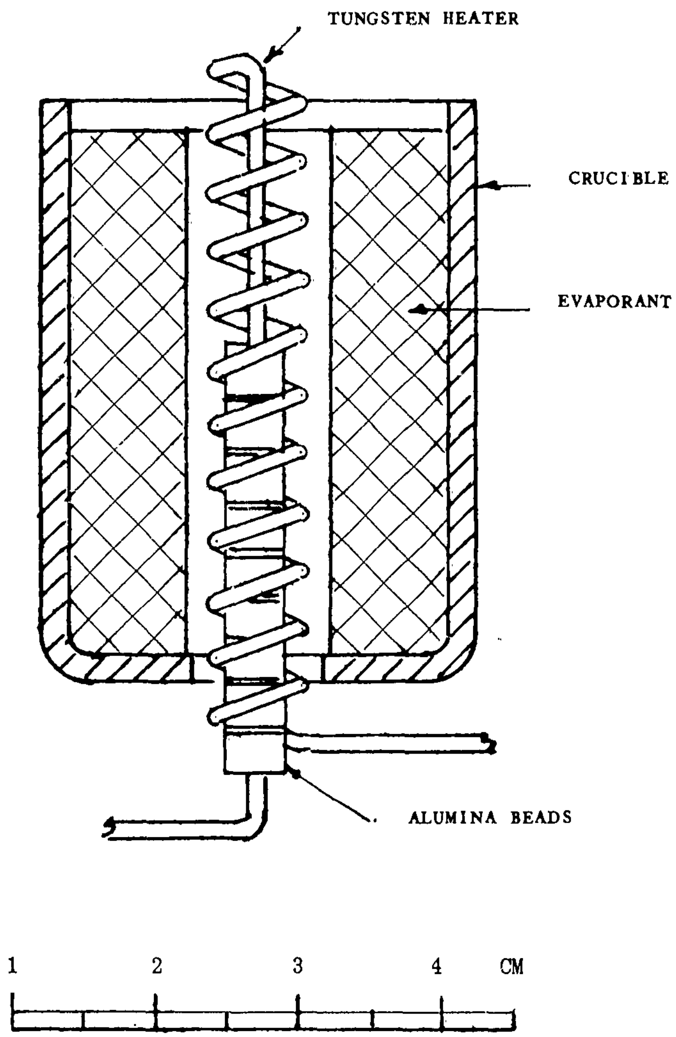

Fig. 3. Evaporation Source for Dielectrics.

tellurium tended to diffuse around the shutter and continued to deposit on the filter. With tellurium it was necessary to switch off the heater current well before the layer had reached the correct thickness, so that at that point the evaporation rate was very slow, and the amount of overshooting could be held to a minimum.

The control system.

There are two ways in which the thickness of the layers of a multilayer system can be controlled. The first method is based on the fact that each time the optical thickness of a layer becomes $\lambda/4$ or a multiple thereof, the transmission of the multilayer stack goes through a minimum or a maximum. This method, which may be called the d.c. method, has the disadvantage that one cannot tell that the signal has reached an extremum until it has been passed. Hence one inevitably tends to overshoot slightly on the layer thickness. This produced a mismatching of the multilayers, and reduced the peak transmission of the filters from the theoretically expected value.

The second, or a.c. method, consists of switching between two wavelengths close to and on either side of the wavelength of the filter. The resulting a.c. signal is synchronously rectified, and becomes zero whenever the layer is a quarter wave thick at the mean wavelength. This, being a null method, is considerably more accurate than the d.c. method. However, because the detected signal is the difference between two nearly equal signals, it requires a considerably higher signal/noise ratio than the d.c. method.

In the infra-red, the signal/noise ratio is limited by the fact that sources of radiation are much weaker than in the visible spectrum. and that the thermal detectors available are many orders of magnitude worse than photo-multipliers.

For these reasons the d.c. system was adopted for this work, and even so it was found that at 20μ, where the source intensity is well down, the signal was barely sufficient.

The final form of the control system is shown in fig.4. The source of radiation is a Nernst filament mounted near the base plate of the vacuum chamber. Light passes from this through the filter and a KRS5 window in the top plate of the chamber to a toroidal mirror. This produces an image of the Nernst filament on the entrance slit of a grating monochromator, set for the desired wavelength. A concave

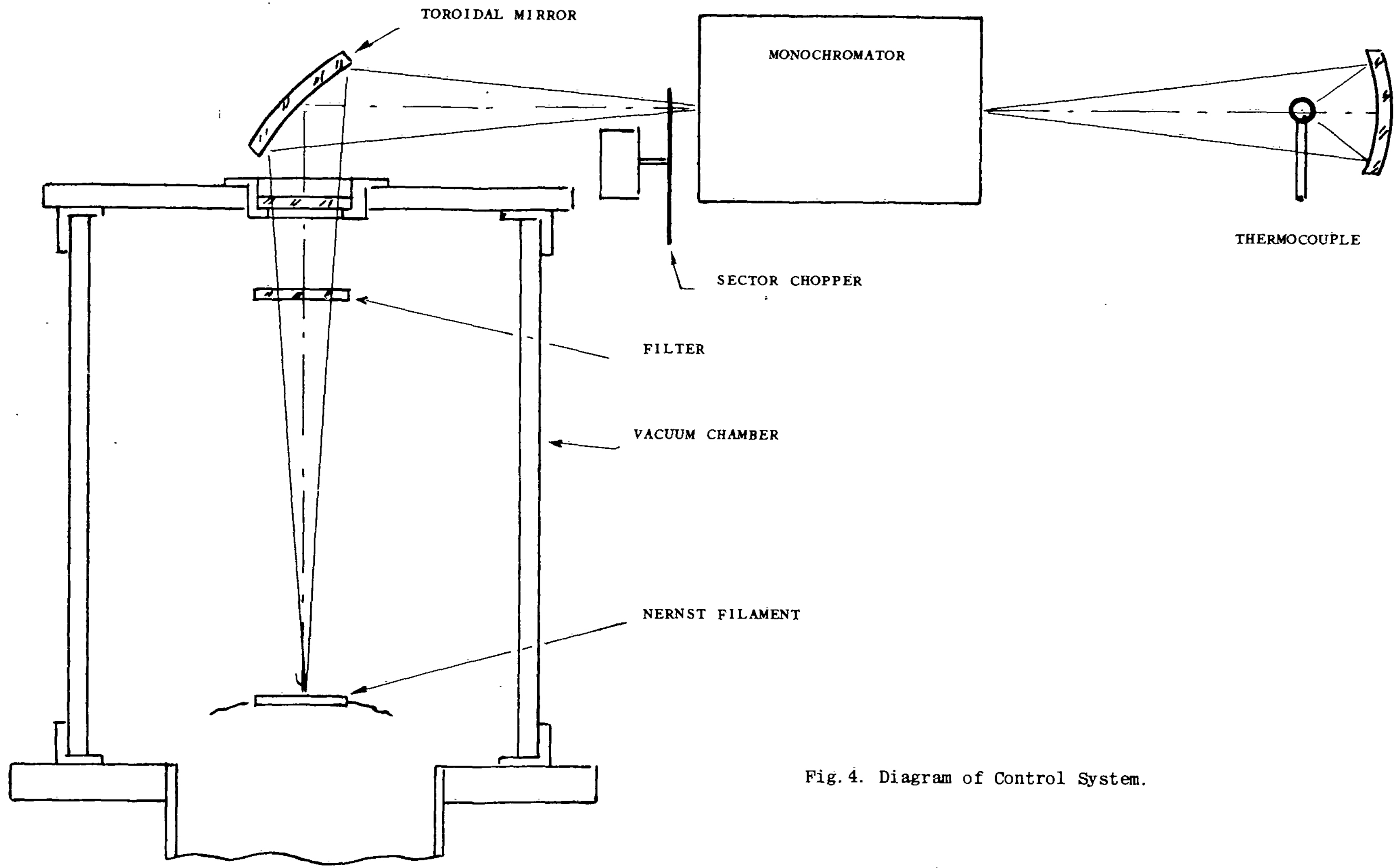

Fig. 4. Diagram of Control System.

spherical mirror focusses the exit slit of the monochromator on to a thermopile (made by Charles M. Reeder, Detroit) with a demagnification of 1/5. A sector chopper interrupted the radiation at a frequency of 10 cycles/sec., and the thermocouple output is amplified by a sharply tuned amplifier (Grubb Parsons, type T.A.10), and displayed on a milliammeter, or pen recorder.

The size of the KRS5 window was not sufficient for the aperture of the monochromator to be filled completely, and a gain in signal by a factor of 4 would be achieved by increasing the size of the window from 25 to 50 mm.

The monochromator originally was a Grubb Parsons type M.1., used with a suitable filter for order sorting, but later the complete double monochromator section of a Grubb Parsons D.M.2. infra-red spectrometer was used.

Initially a Golay detector was employed, but it was found that compared with the Reeder thermocouple this was very noisy, and tended to drift; it was therefore abandoned.

Filter production

A multilayer filters can be characterized by the following parameters:

1) Wavelength of transmission peak.

2) Peak transmission.

3) Bandwidth at half intensity.

4) Suppression (Transmission on either side of pass band - ideally zero).

It was found that with the d.c. control system the peak wavelength could be repeated to better than 1% at any wavelength. The actual wavelength naturally depends on the accuracy of calibration of the control monochromator.

The peak transmission of a filter should be 100%, if there is no absorption in the layers, and the layers are perfectly matched (allowing for reflection losses on the back surface of the substrate). None of the filters produced showed a transmission approaching the ideal. In part this was due to the presence of absorption in the tellurium layers. Scanning a single tellurium film showed that there was absorption of the order of 3%. This may be caused by impurities in the tellurium, which was only of reagent (99.9%) purity. An improvement would probably result from the employment of zone refined material - for which however no source of supply could be found. In part the loss of transmission was also due to mismatching of the layers. This was apparent from the fact that filters of identical construction often showed widely different values of peak transmission. In general, values of transmission greater than 60% were easily obtained.

The halfwidth and suppression of a filter depend on the effective reflectivity of the two multilayer stacks of the filter, and this reflectivity depends on the number of layers in each stack, and on the difference of refractive index between alternate layers. In the presence of absorption the number of layers is limited by the decrease of peak transmission, and it was found that the maximum number that could be used to advantage was 5 layers in each stack. A filter of this construction has a relative halfwidth ($\delta\lambda/\lambda$) of approximately 1/80, and transmission in the suppression region is sensibly zero. Peak transmission in this case is about 45%. Of course it is always possible to trade halfwidth for transmission by reducing the number of layers. As regards refractive index difference, the best combination should be - and was found to be - tellurium/NaF.

In addition to the normal filters of the type stack/spacer/stack, a number of double half wave filters were made successfully (Smith, D.S., [4]).

These filters are characterised by an approximately rectangular pass band of relative half width $\delta\lambda/\lambda = 1/15$, very good peak transmission and suppression.

A representative selection of transmission curves is given in figs. 5 - 15.

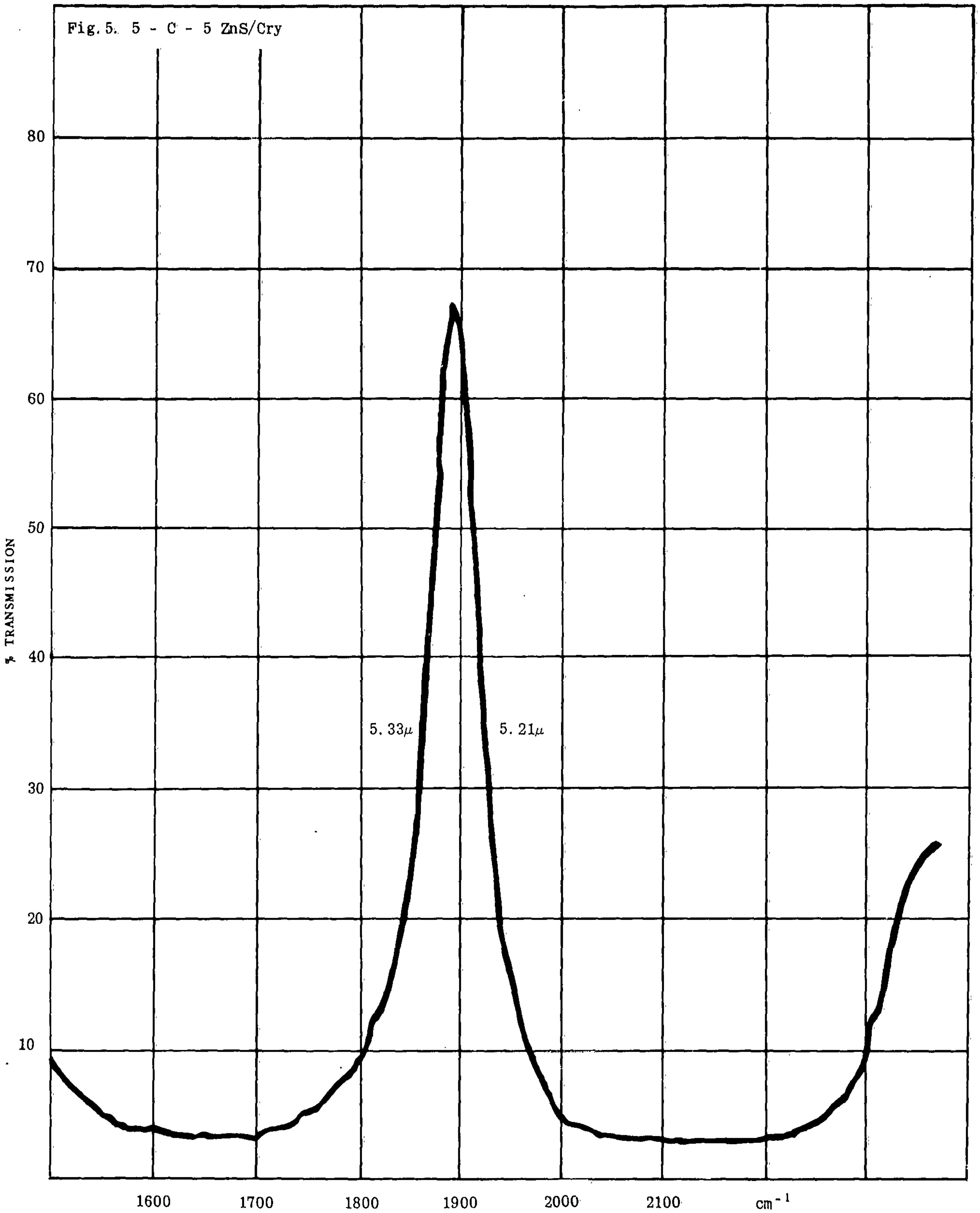
Fig. 5. 5 - C - 5 ZnS/Cry
% TRANSMISSION
80
70
60
50
40
30
20
10
5.33μ
5.21μ
1600
1700
1800
1900
2000
2100
cm⁻¹

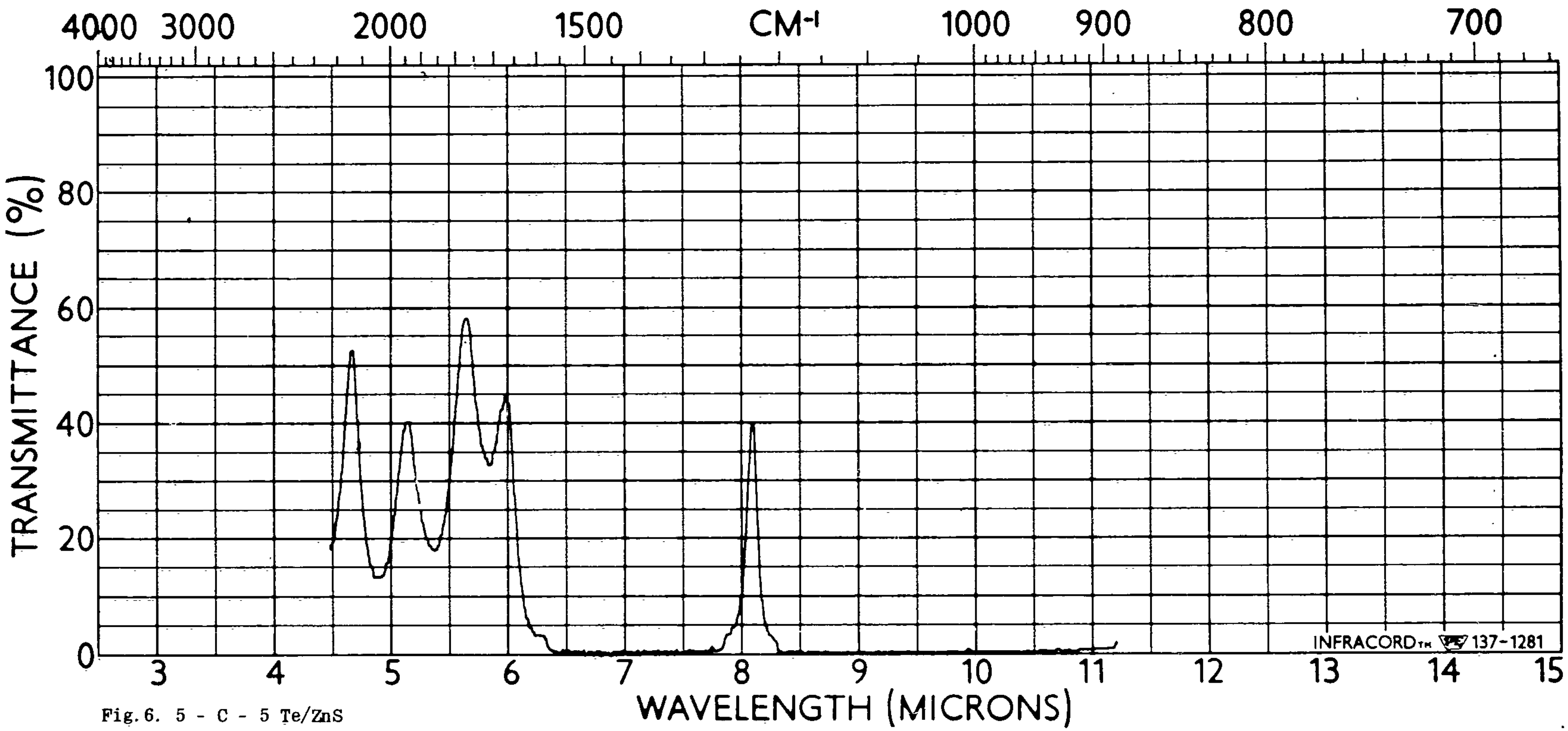

Fig. 6. 5 - C - 5 Te/ZnS

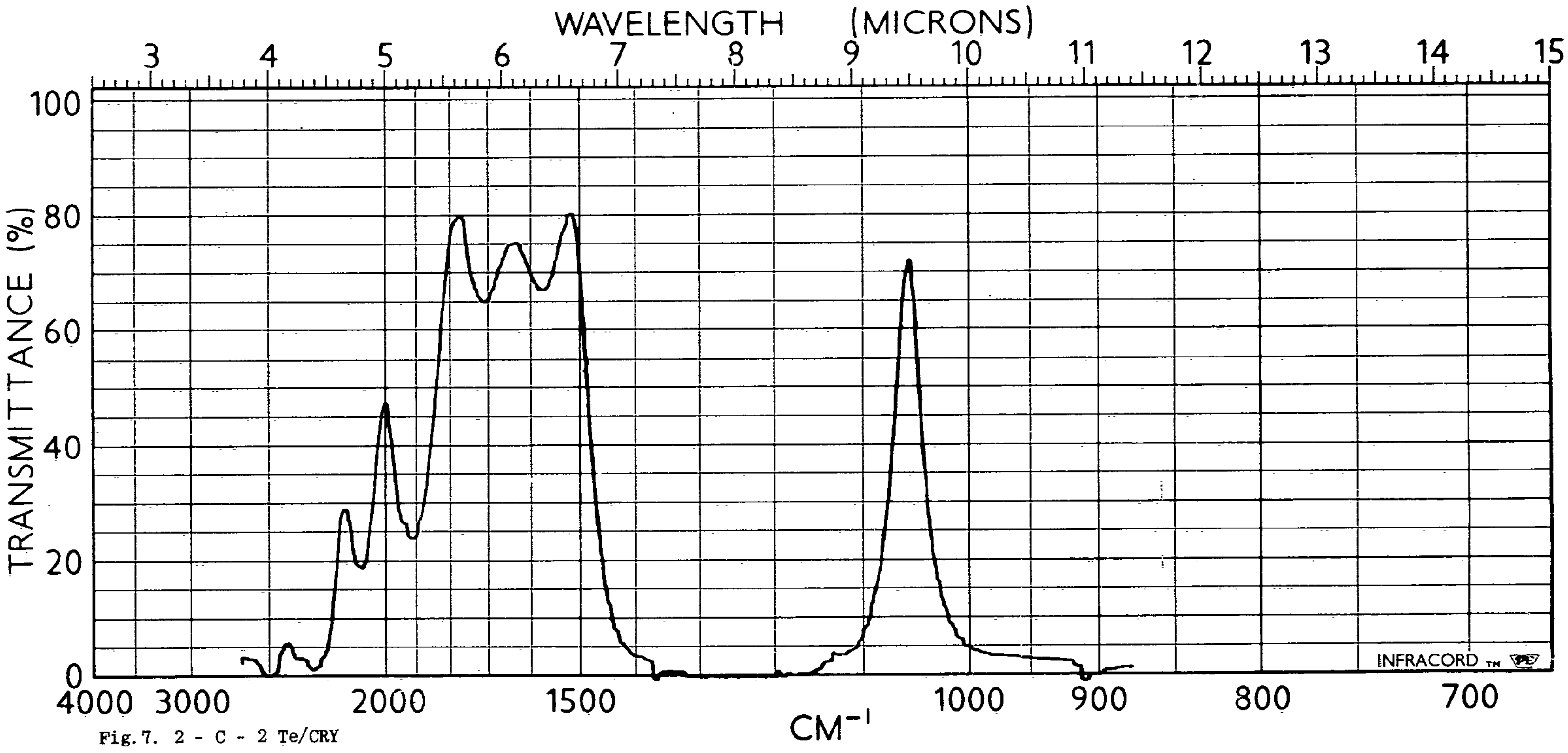

Fig.7. 2 - C - 2 Te/CRY

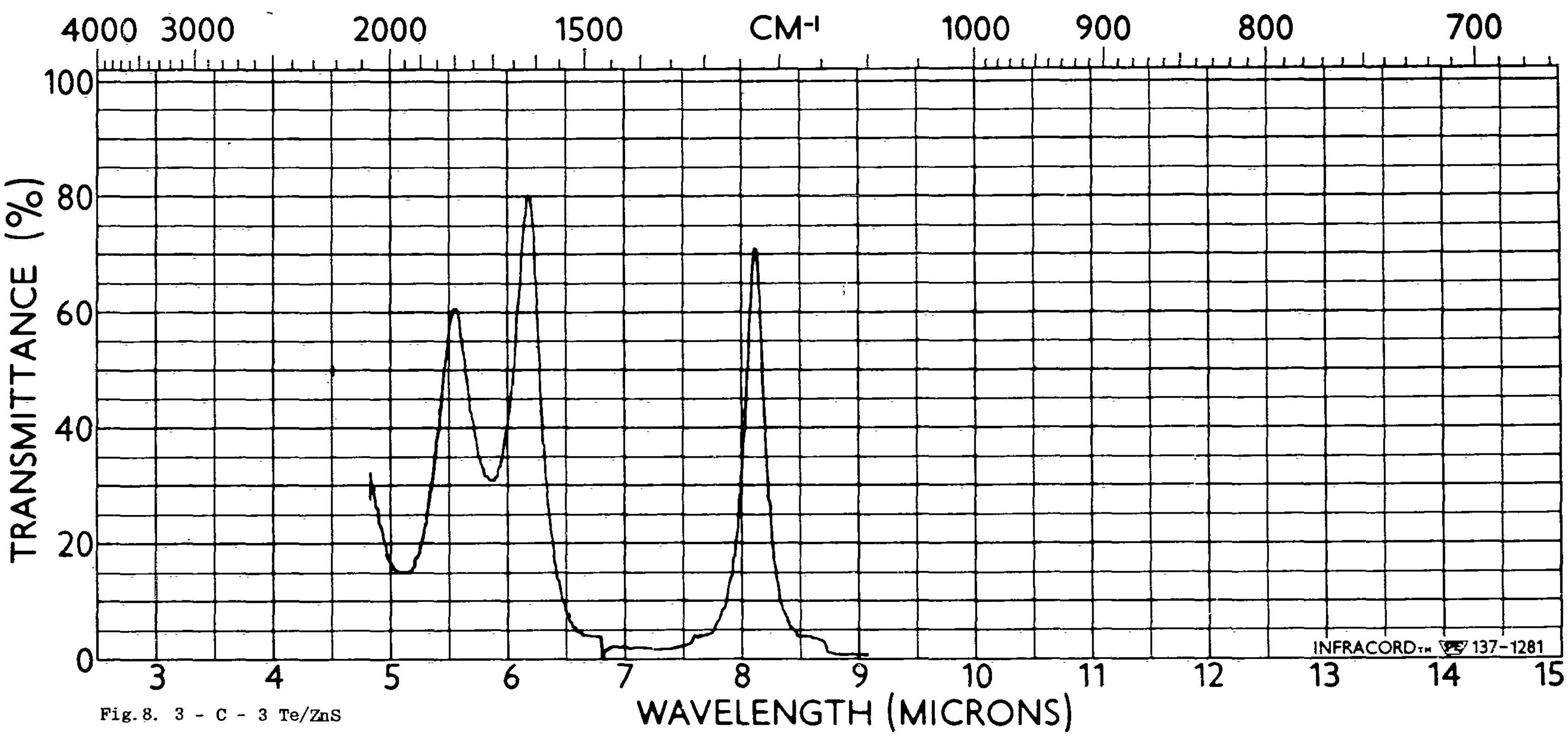

Fig. 8. 3 - C - 3 Te/ZnS

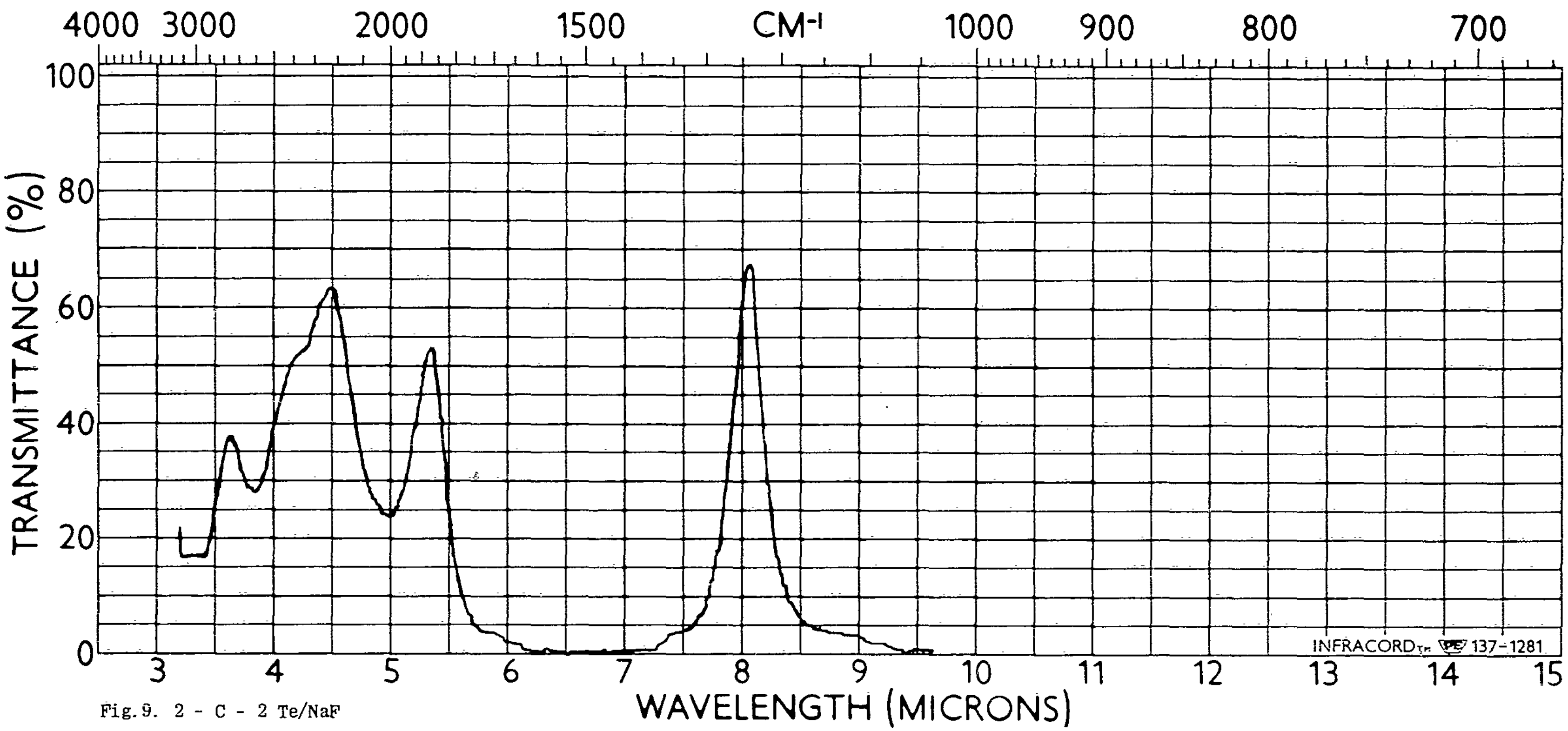

Fig.9. 2 - C - 2 Te/NaF

3 - C - 3

Te/KB

Fig. 10. 3 - C - 3 Te/KBr

Centred on 760 cm^{-1} (13.15μ)

Half Width 27 cm^{-1} (0.46μ),

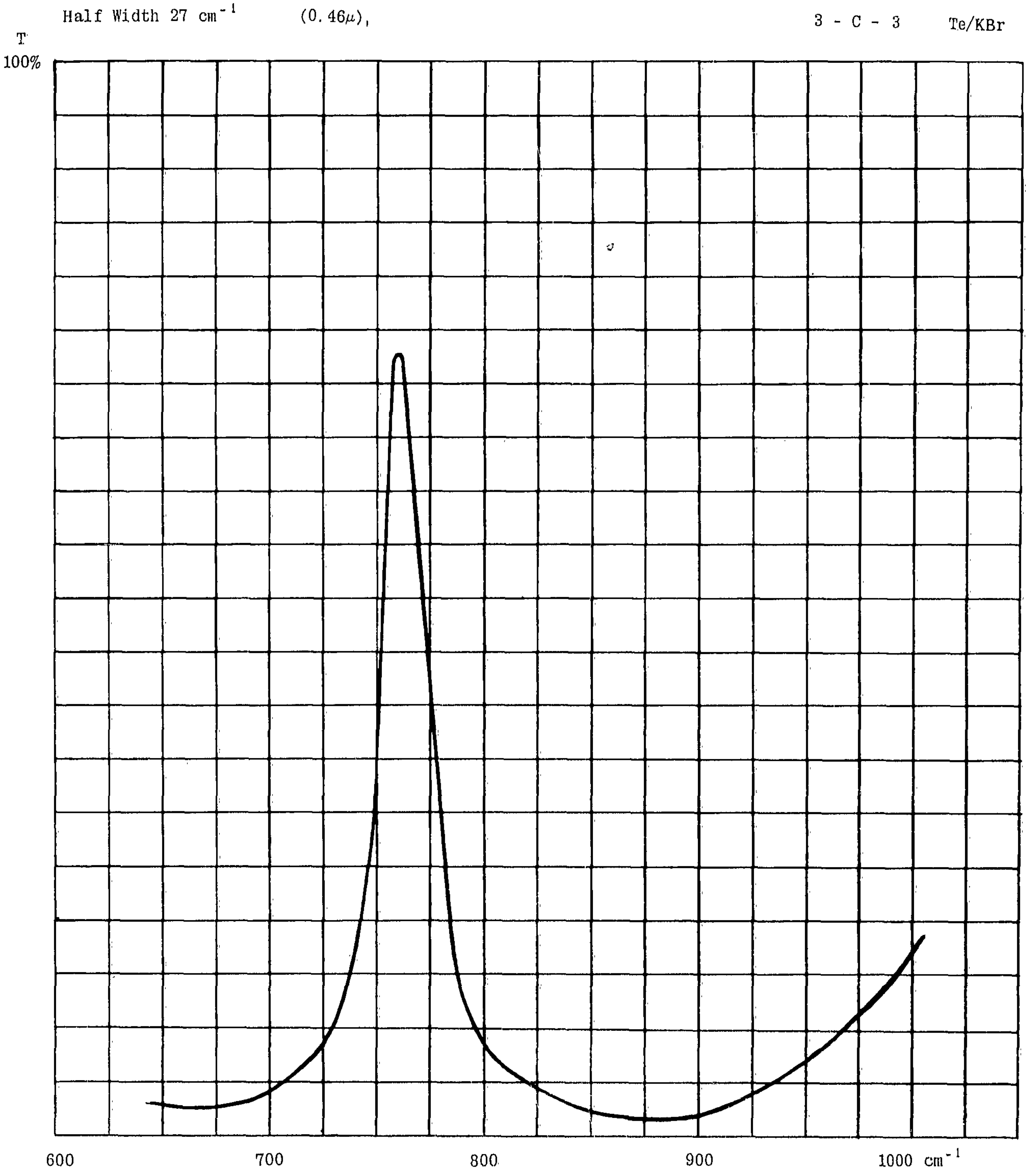

Fig. 11. 2 - Te - 2

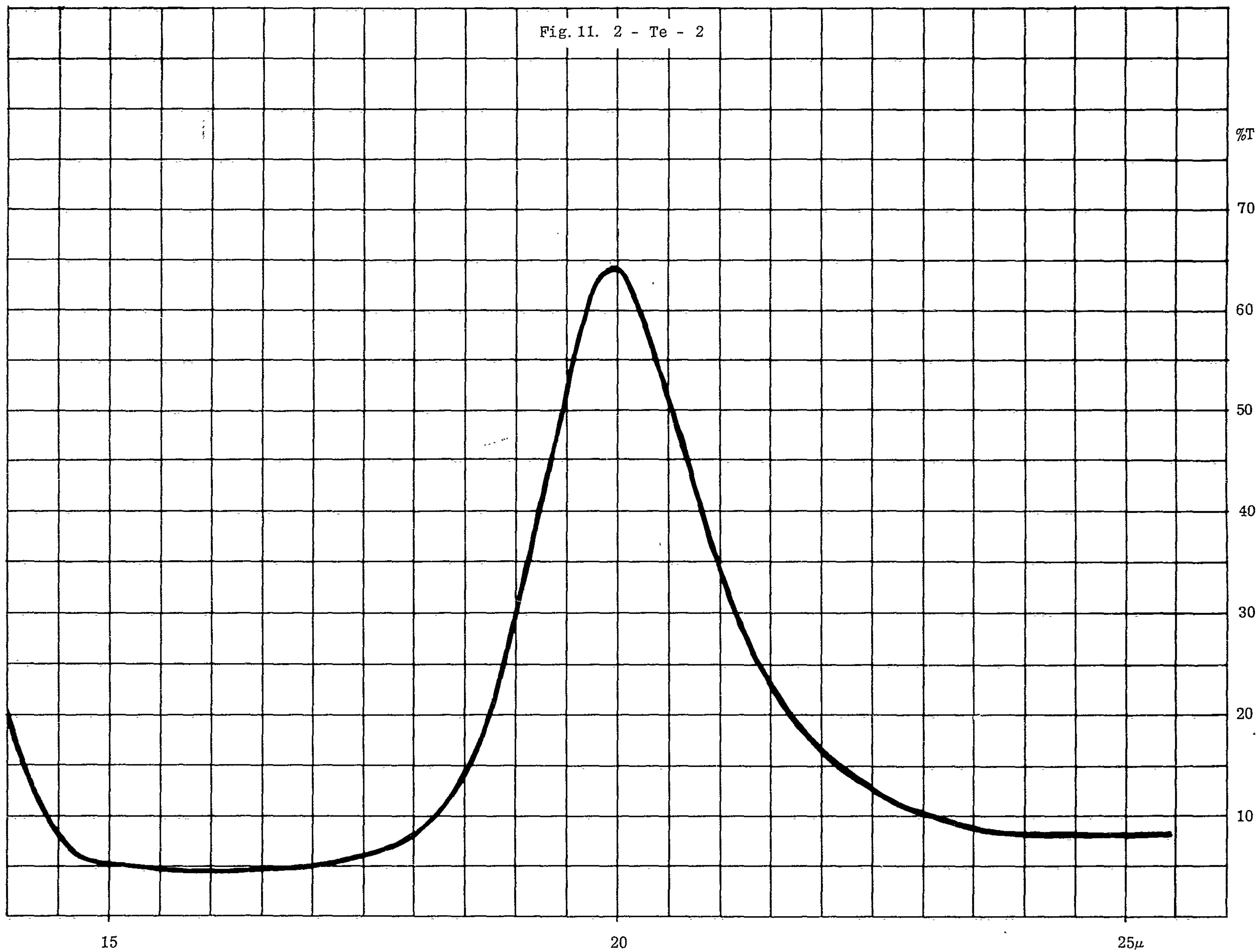

Fig. 12.
3 - KBr - 3
Peak Transmission 78%
Half Width 32 cm^{-1}
At 498 cm^{-1}

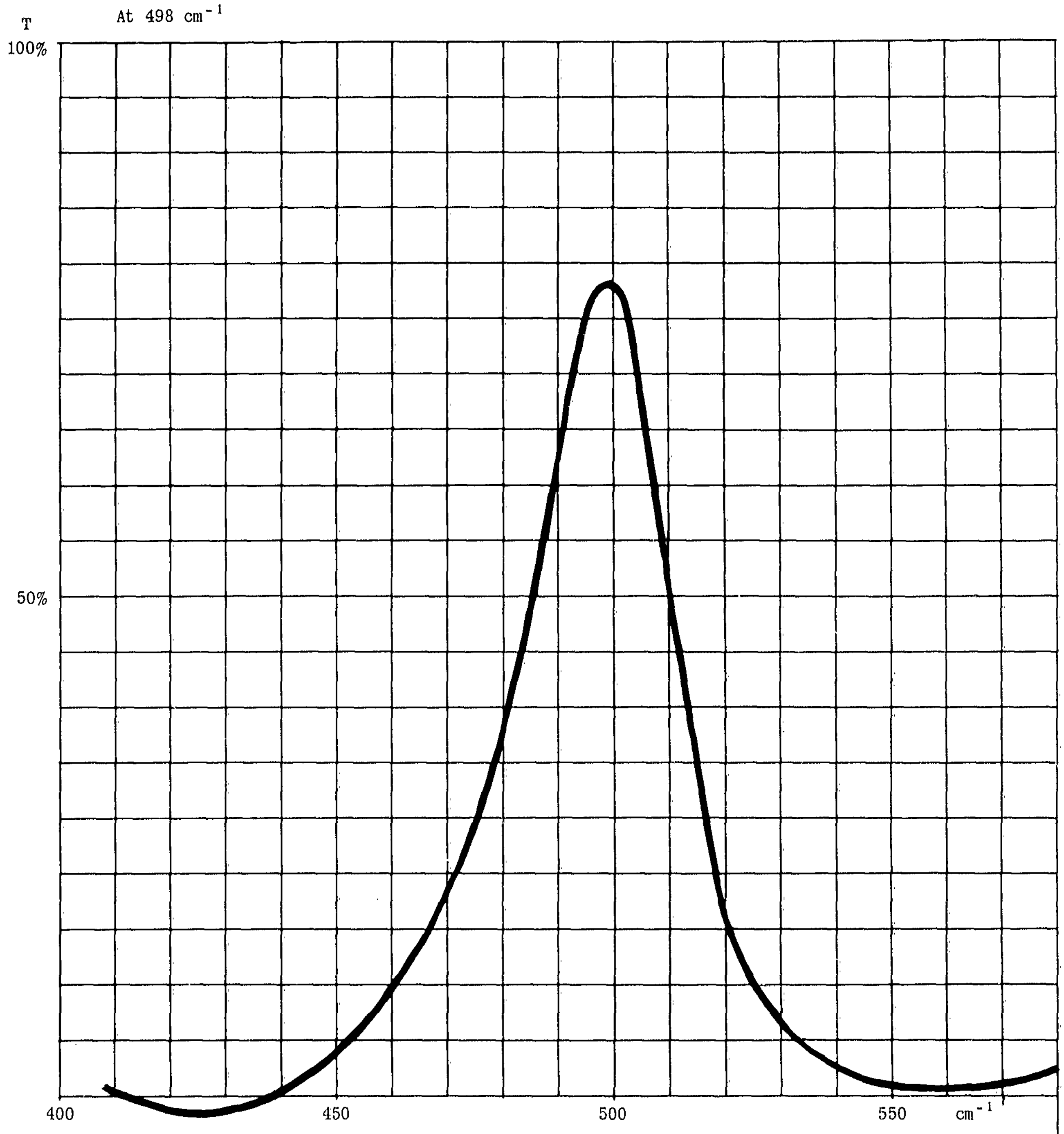

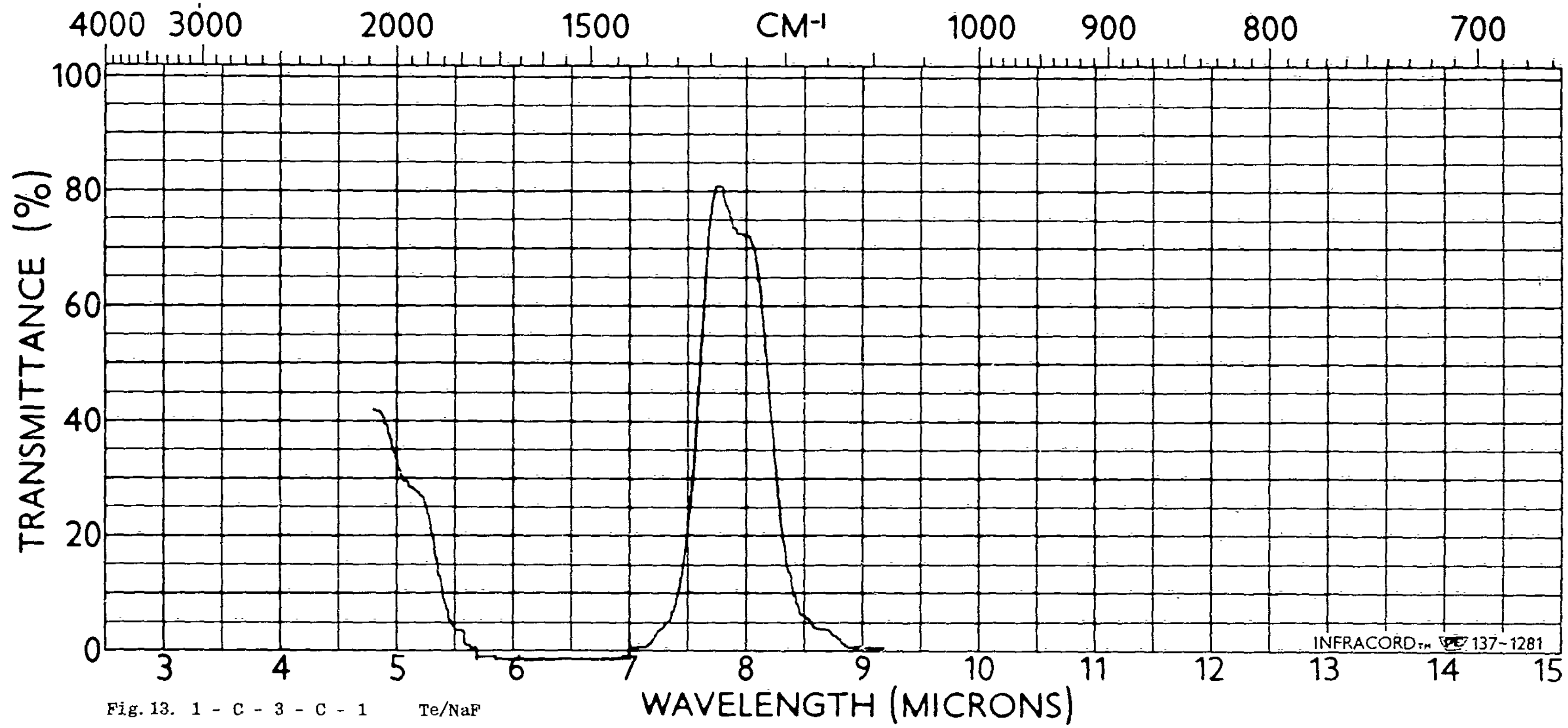

Fig. 13. 1 - C - 3 - C - 1 Te/NaF

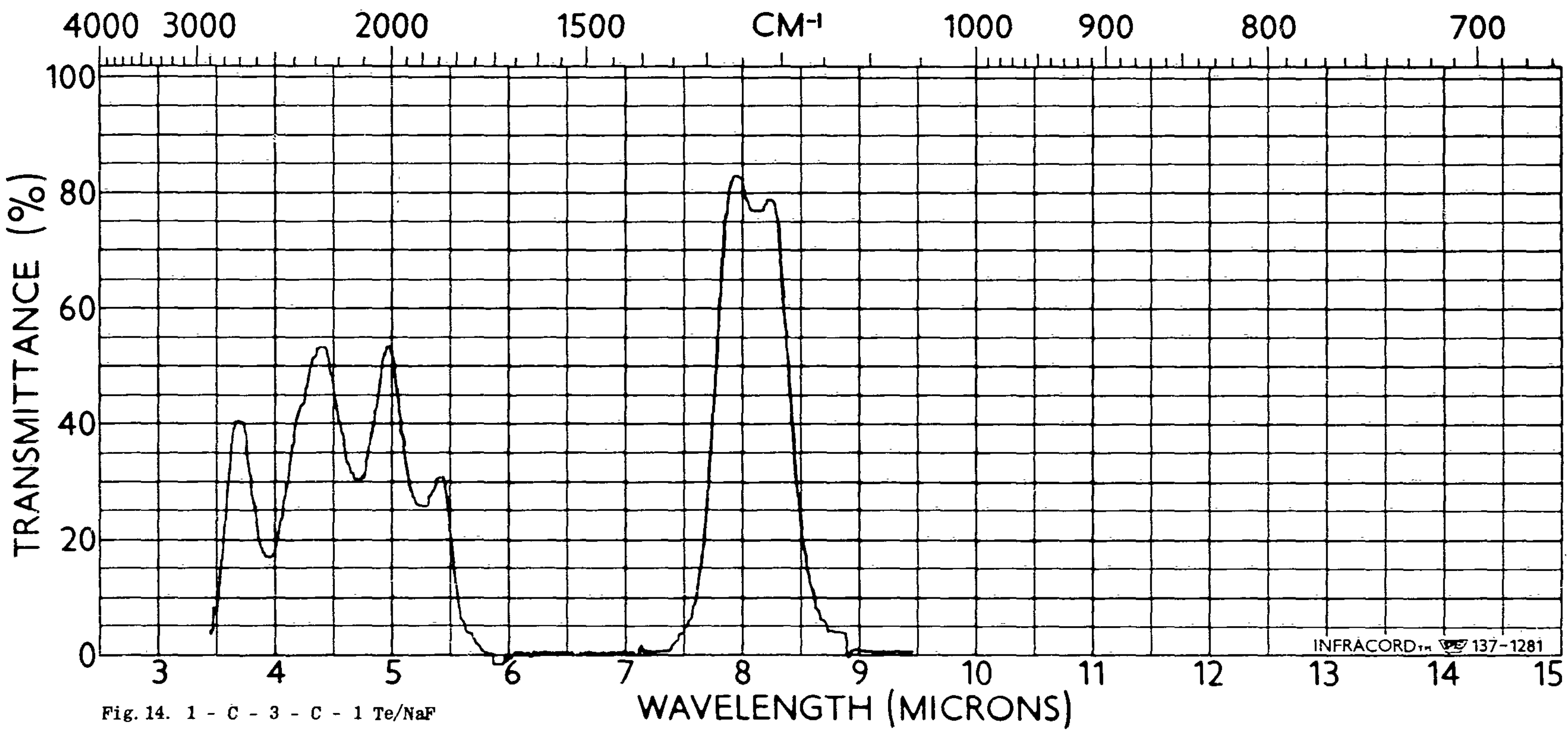

Fig. 14. 1 - C - 3 - C - 1 Te/NaF

Fig. 15.

Double Half Wave Filter 1 - C - 3 - C - 1 Te/KBr

Centred on 765 cm^{-1} 13.1μ

Half Width 105 cm^{-1}

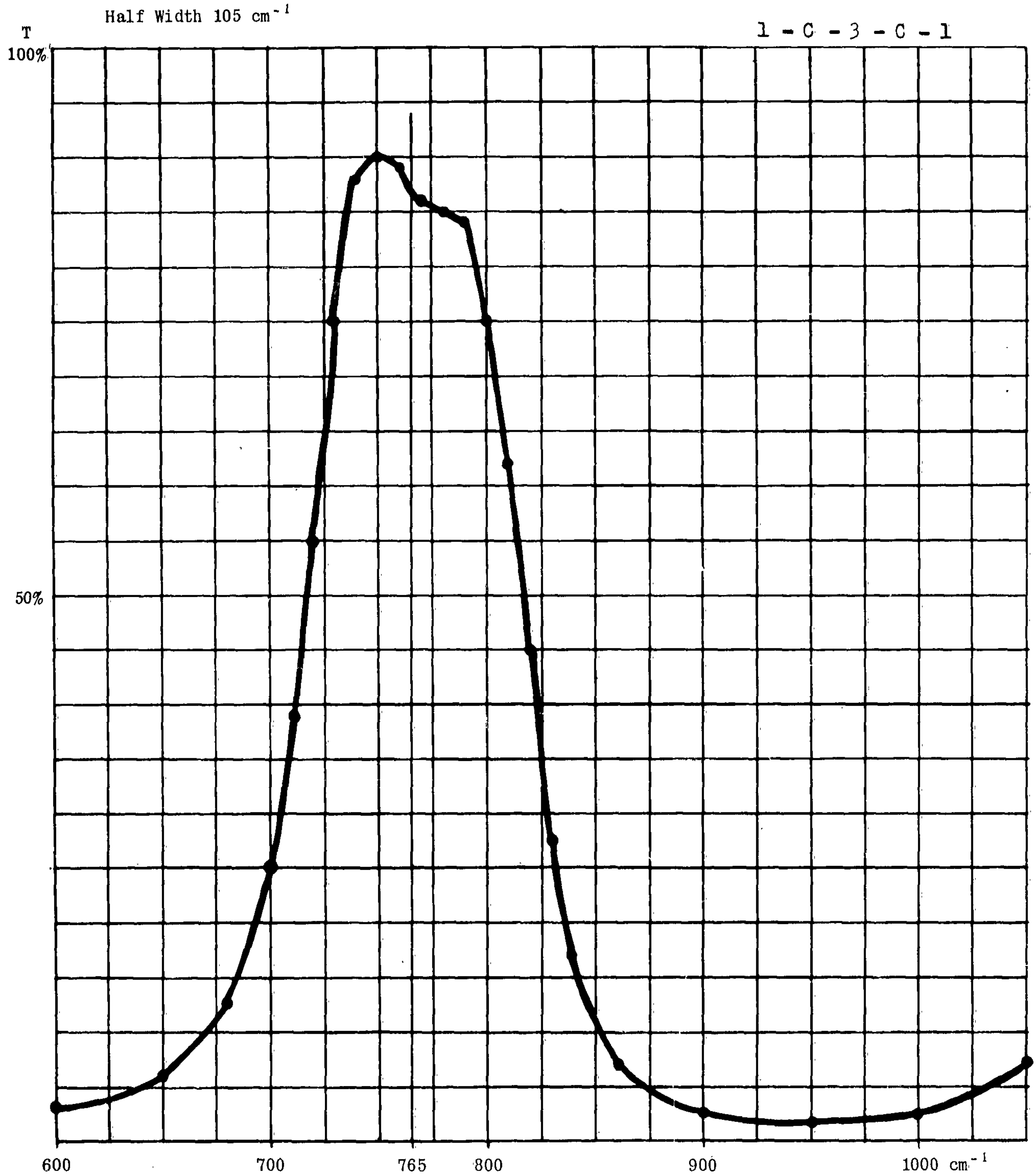

II. DESIGN OF AN INFRA-RED PHOTOMETER

The photometer was to be used at the Newtonian focus of the 122-cm F/5 telescope at Asiago. The lunar image at this focus is approximately 5 cm. in diameter; therefore to obtain a spatial resolution of approximately 10 secs of arc, a scanning aperture of the order of 0.3 mm diameter is needed.

Previous workers who had used this telescope had found that there is an appreciable amount of differential flexure between the telescope itself, and the guiding telescope, when guiding is done for a prolonged period. Hence it was considered essential in the present case, where the telescope has to be kept pointed at a definite, known area of the moon for a considerable period, to use the Newtonian image itself for guiding.

An estimate of the energy flux to be expected can be obtained by assuming the moon to be a black body at a temperature of 0°C (this figure is taken as the lower limit to which, in the first instance measurements will be made - it is approximately correct for the terminator region). Using the full width of the atmospheric window from 8-13μ, and assuming a transmission efficiency of the telescope and photometer of 50% (this figure must necessarily be assumed, depending on the number of reflections taking place, which is known, and on the state of the coatings of the mirrors, which is not known, especially in the case of the telescope), a figure of approximately 5×10^{-7} watts per cm^2 of scanning aperture is obtained. For the above mentioned spatial resolution of 10 secs of arc, i.e. a scanning aperture of 0.3 mm diameter, the available energy flux is 3.5×10^{-10} watts. When the narrow band filters (bandwidth approximately 1μ) are in use, this figure must be divided by approximately 5.

Choice of detector

For the spectral region under consideration possible detectors are the following:

1) Thermocouple

2) Golay cell

3) Superconducting bolometer

4) Doped semi-conductor (germanium) detector

Choice of 3) and 4), although superior to 1) and 2) from the point of detectivity and speed of response, were ruled out because of the difficulty of providing the necessary supply of liquid helium at the observatory. As far as thermocouple and Golay cell are concerned, the latter has in principle a higher detectivity (D*). When attempting to use it for controlling the evaporation process in filter making, the author found that it suffered from long term drifts, and microphonic effects, which would make its use on the telescope difficult.

Hence the thermocouple is left as the only practical possibility. Following Sinton [9] it was decided to use two thermocouples, arranged in such a manner that the radiation falls on to the receivers of the two thermocouples alternately. The thermocouples are connected to the amplifier in series-opposition. This should lead to a gain of 2x in signal, and an increase in noise by a factor of $\sqrt{2}$, i.e. to an overall gain in S/N ratio of $\sqrt{2}$.

The vacuum thermocouples were manufactured by Messrs. Charles M. Reeder, of Detroit, Mich. The radiation receivers were 1/2 mm diameter. The detectivity of these thermocouples (D*) may be assumed to be of the order of 2×10^9. No explicit figure for this could be obtained from the manufacturers who only gave a figure for the sensitivity of 10-12 μ V per μ WATT.

A diagram of the optical layout of the instrument is shown in Fig. 20. The image of the moon formed by the telescope lies in the plane of the diaphragm A. This diaphragm consists of a disc of aluminized perspex (poly-methylmethacrylate), with a central hole defining the area of the moon the instrument looks at. The diaphragm disc is slightly inclined from the optical axis, and the image of the moon can be viewed by means of the guiding miscroscope B. In this miscroscope the scanning aperture appears as a black spot, which can be positioned on a selected area of the lunar disc.

Interchangeable scanning discs with the following apertures are provided:-

No.	Diameter	Angular subtense at focus
1	0.19 mm	6.2″
2	0.34 mm	11″
3	0.625 mm	20″
4	1.00 mm	32.5″
5	1.5 mm	49″

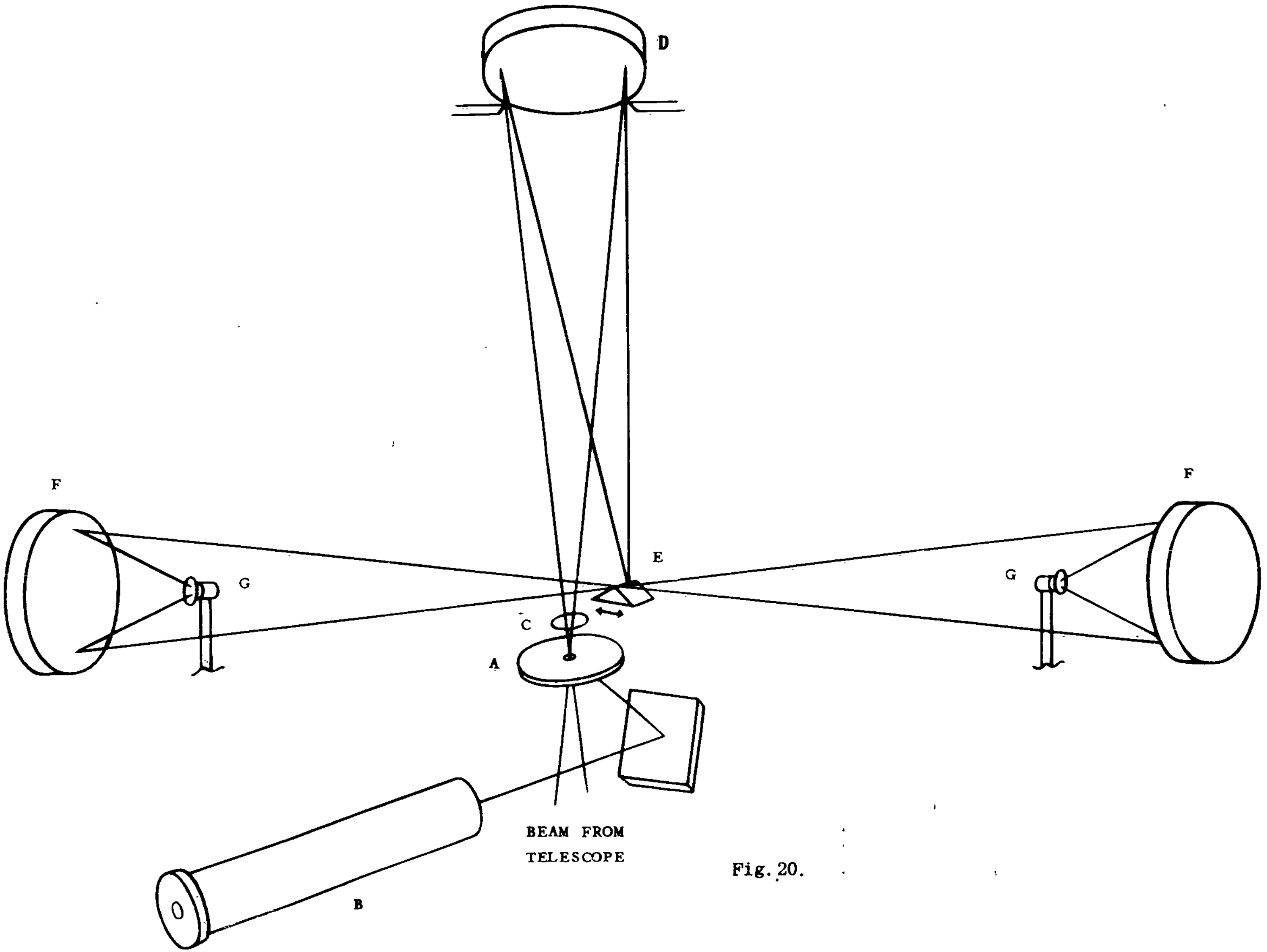

Fig. 20.

The resolving power of the telescope at a wavelength of 10μ is 0.06 mm or 2secs of arc, i.e. well below the smallest aperture size. In actual practice it was found that the energy transmitted by aperture no. 1. was so small that unduly long integration times were required, and this aperture was not used.

After passing through the aperture the radiation is re-focussed by the concave mirror D. fig (20) A BaF_2 field lens C images the primary mirror of the telescope on to a diaphragm immediately in front of the mirror D. The size of this diaphragm is slightly less than the image of the telescope primary, so that the rest of the instrument cannot see the interior of the telescope tube. The lens C also serves as a filter to remove radiation of wavelength longer than 13μ.

Mirror D re-images the scanning aperture on the edge of the prism E. The two faces of this prism are aluminized, and the prism is caused to reciprocate at 10 cycles/sec. by a synchronous motor. Thus the radiation is alternately reflected from the two faces of the prism, and is condensed onto the thermocouples G by the mirrors F. Two indium antimonide filters serve to cut out radiation of wavelength shorter than 7.5μ. These filters are bloomed to give maximum transmission at 9.5μ, and their transmission curves are shown in fig. 21. Narrow band interference filters in plug-in mounts can be inserted between the lens C and the mirror D.

The signal from the thermocouples is applied via an impedance matching transformer to the input of a Grubb Parsons type TA/10 amplifier. The circuit of this amplifier is shown in fig. 22. It is of conventional design, consisting of a low noise pre-amplifier stage V_1, two stages of triode amplification V_2, and two stages V_3 and V_4 with negative feedback loops incorporating 'bridge T' networks tuned to the chopping frequency of 10 cycles/sec, giving a bandwidth of 1 cycle/sec. V_5 is a selfbalancing phase splitter, providing a push-pull signal to the two diodes V_6 and V_7. V_8 is a balanced cathode follower, supplying the output signal to a penrecorder via a suitable attenuator.

This amplifier was modified in a number of ways, as follows:-

1) The (continuously variable) gain control R_{10} was replaced by a 10 position switch, and a resistor chain, giving 9 values of gain in the approximate ratio 2/1. (The 1st switch position corresponds to zero gain). The exact ratios of the gain steps are:-

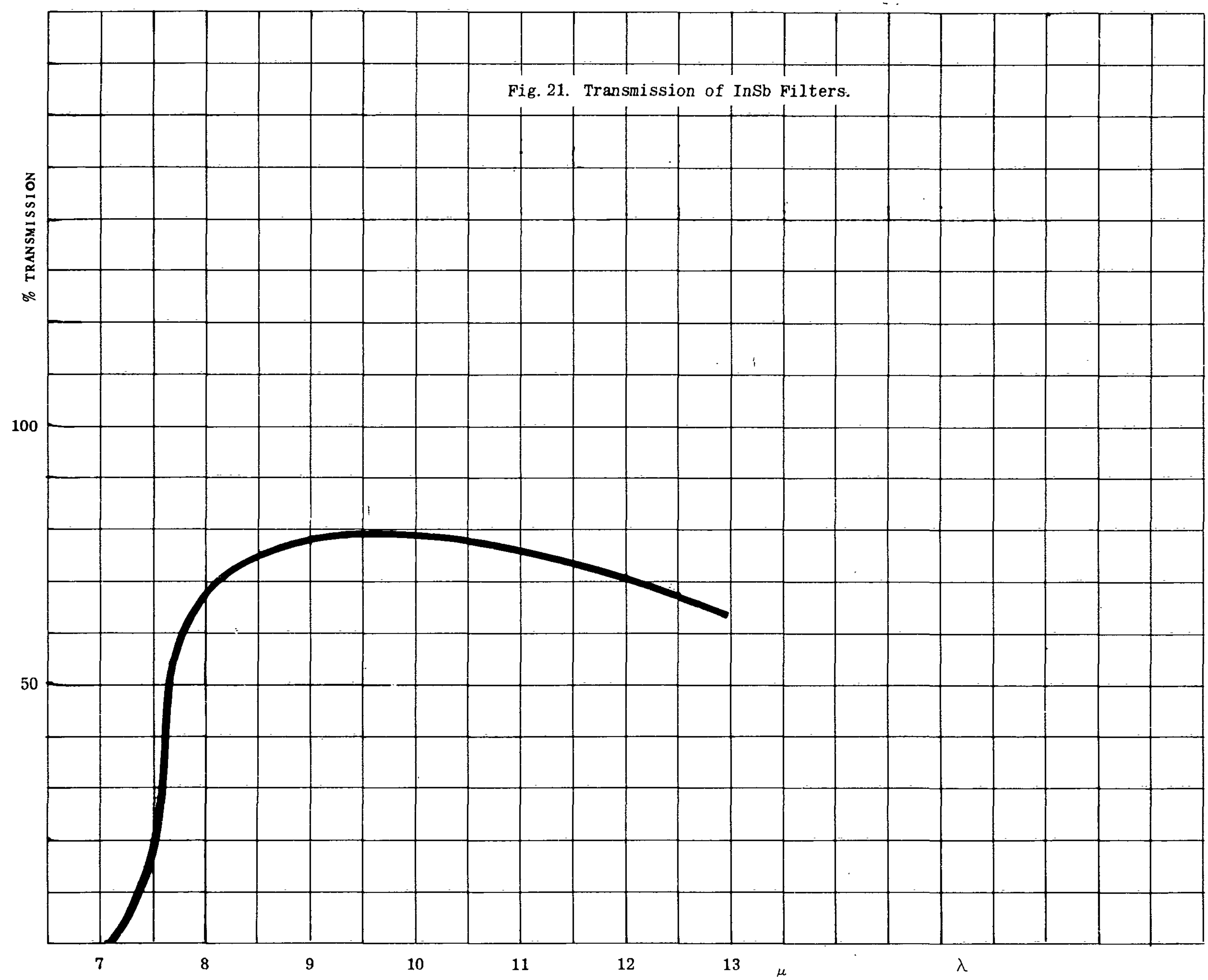

Fig. 21. Transmission of InSb Filters.

Steps	Ratio
10/9	1.85
9/8	2.00
8/7	1.93
7/6	1.97
6/5	2.08
5/4	2.20
4/3	2.19
3/2	1.97

2) In order to be able to use longer integration times, a time constant (RC) network was incorporated in the amplifier. By means of a 6 position switch time constants of 0.7, 2.0, 7, 12, 16, and 21 seconds could be selected.

3) By means of a switch the built in (non-phase sensitive) diode rectifier could be cut out, and replaced by an external, phase sensitive rectifier. This rectifier was to be operated by the synchronous motor driving the chopping prism. A phase sensitive rectifier is necessary because the instrument measures the difference in temperature between the object it looks at, and the ambient temperature. Without phase sensitive rectification there is no way of telling whether the temperature measured is higher or lower than the ambient temperature. In practice it was found that the phase sensitive rectifier, which consisted of cam operated contact springs, was rather noisy, and caused signal drifts. The phase sensitive rectifier was therefore only used to find the sign of the temperature difference, the actual magnitude of the difference being determined using the diode rectifiers. In either case the instrumental zero corresponds to the ambient temperatures, and fluctuations in this temperature will manifest themselves as a zero drift. A mercury thermometer attached to the instrument was read at frequent intervals, and the readings noted on the recorder charts so as to guard against this effect.

To calibrate the instrument, a slide can be inserted, which carries a black body at a known temperature. By means of two mirrors the cavity of the black body is imaged on to the scanning aperture of the instrument. Two mirrors were chosen for this purpose so as to keep the total number of reflections during calibration the same as during measurement (where two reflections take place at the primary and Newtonian mirrors of the telescope).

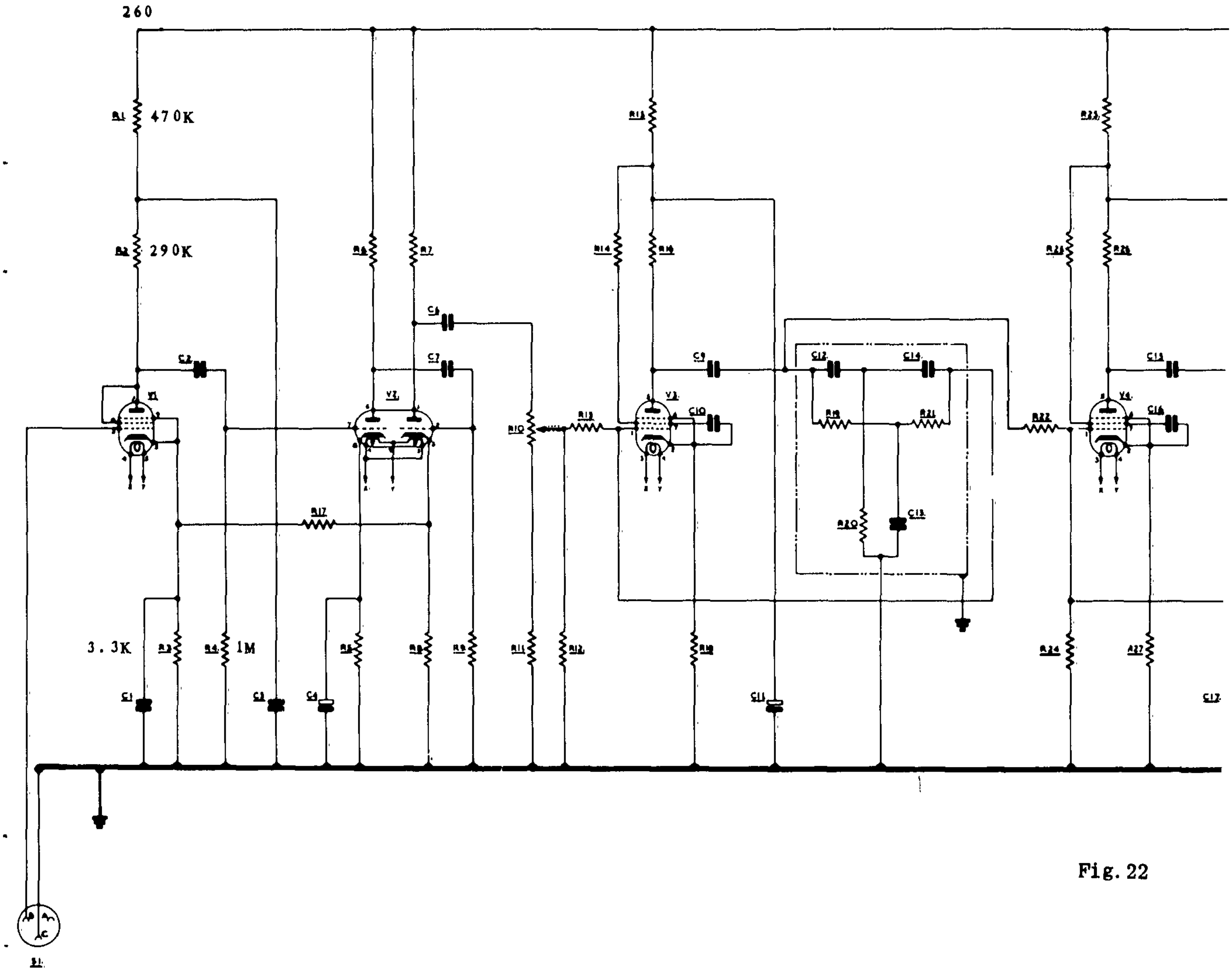
260
R1 470K
R2 290K
3.3K
R3
R4 1M
V1
V2
V3
V4
C1
C2
C3
C4
C6
C7
C9
C10
C11
C12
C13
C14
C15
C16
C17
R6
R7
R8
R9
R10
R11
R12
R13
R14
R15
R16
R17
R18
R19
R20
R21
R22
R23
R24
R25
R26
R27

Fig. 22

1

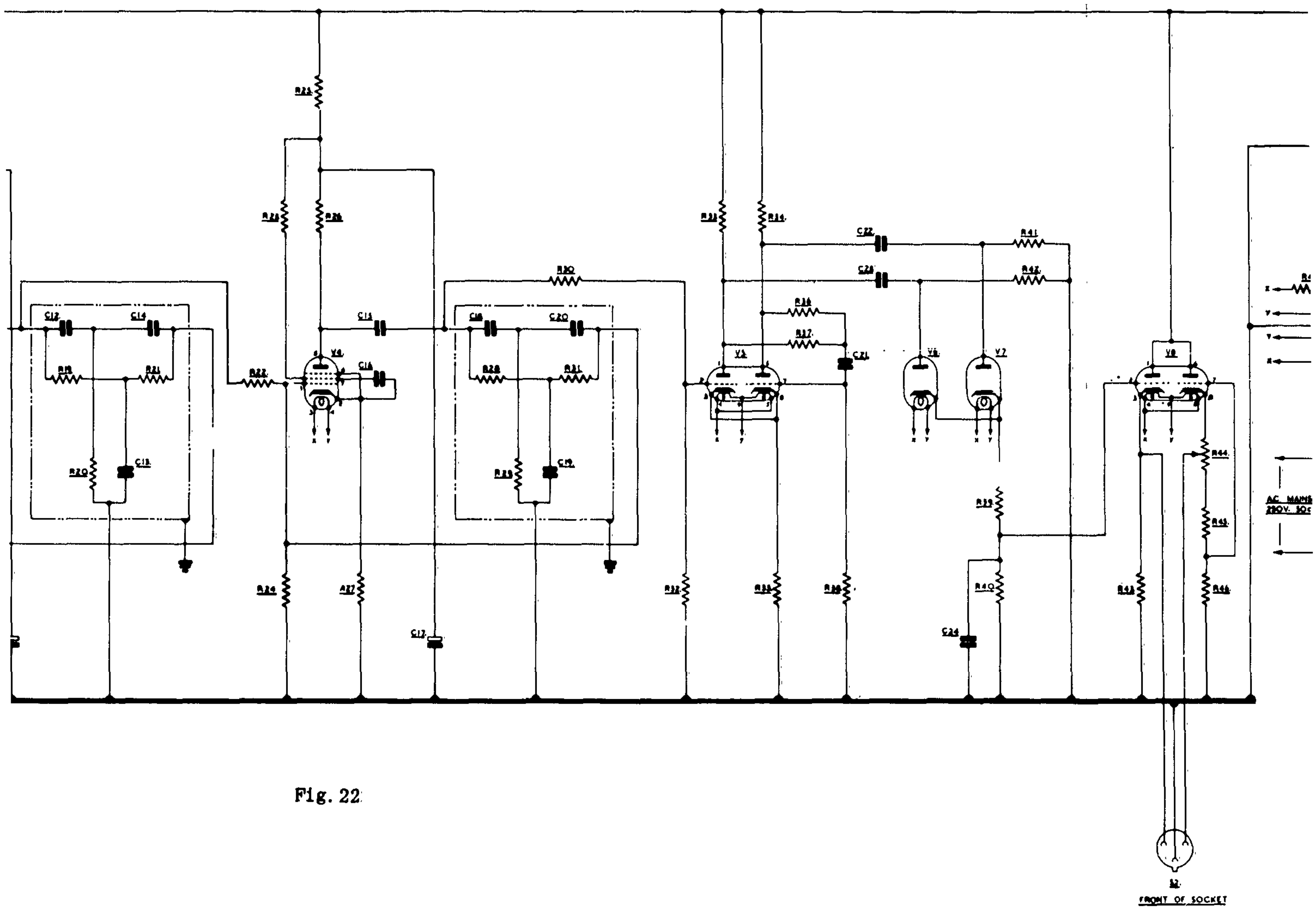

Fig. 22

2

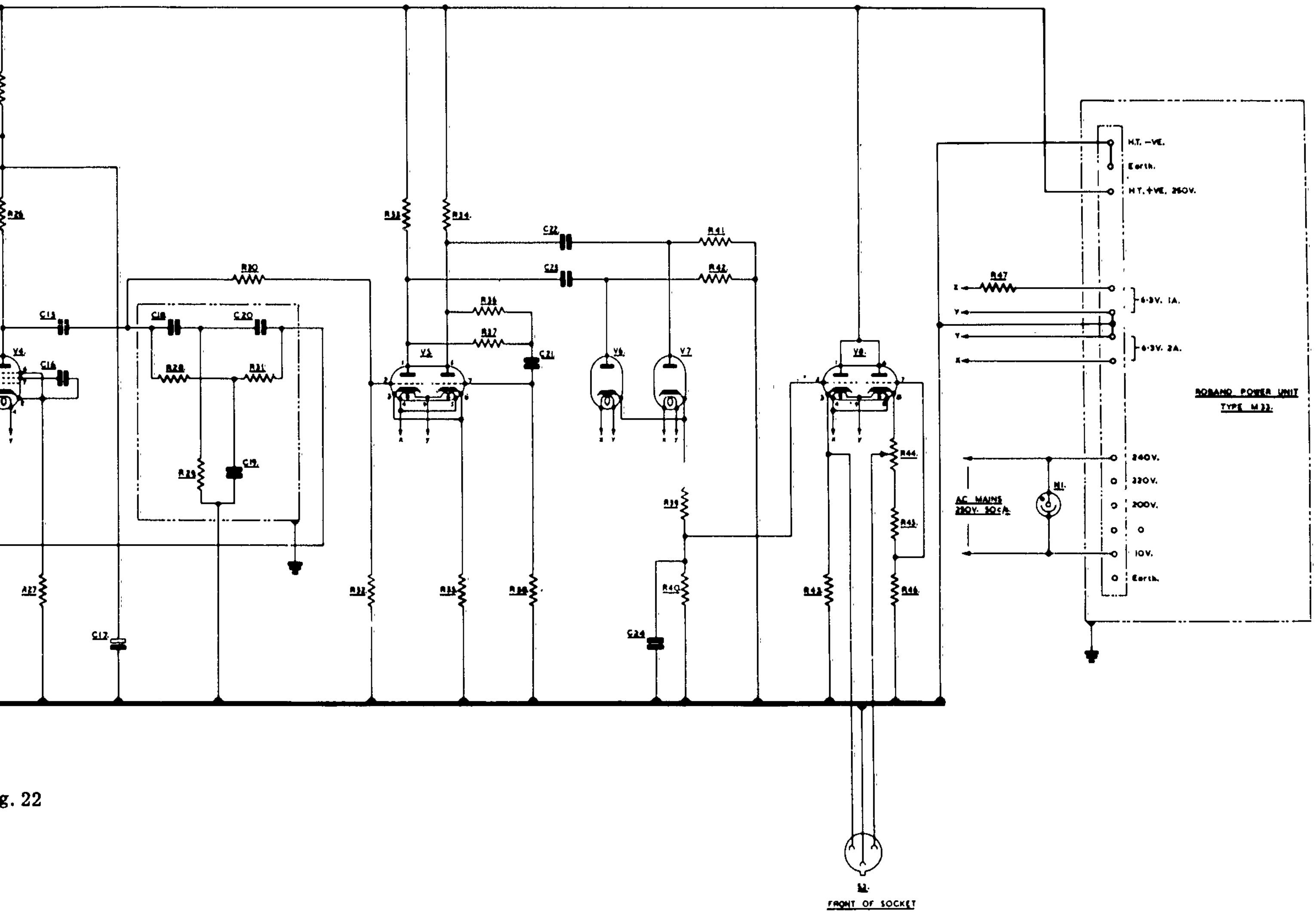
H.T. –VE.
Earth.
H.T. +VE. 250V.
R47
6·3V. 1A.
6·3V. 2A.
ROBAND POWER UNIT
TYPE M 33.
240V.
220V.
200V.
0
10V.
Earth.
AC MAINS
230V. 50c/s.
N1.
V4.
V5.
V6.
V7.
V8.
R26
R30
C15
C16
C18
C20
R28
R31
C19
R27
C17
R32
R33
R34
R36
R37
C21
C22
C23
R41
R42
R44
R45
R46
R43
R40
C24
FRONT OF SOCKET

g. 22

3

Three black bodies were provided, which could be interchanged in a suitable fitting on the slide. One of these black bodies carried an internal heating spiral, so that when filled with water it could be raised to any temperature up to 100°C. The other two black bodies have no heating arrangements, and are intended to be filled with melting ice (0°C), and a solid CO_2-Acetone mixture (-78°C).

Various views of the instruments and its components are shown in figs. 23, 24, 25 and 26.

Fig. 23. shows the instrument mounted at the Newtonian focus of the Asiago telescope. The guiding microscope is visible in the centre of the photograph. For the sake of clarity all cables etc. had been disconnected.

Fig. 24. is a view of the instrument with its cover removed. The main optical components and the thermocouples (covered by dessicated sleeves) are readily seen.

Fig. 25. Shows the chopping prism, mounted on a parallel spring strip suspension, and driven by an eccentric crankpin engaging in a slot in the prism mount. The synchronous driving motor at the left of the photograph is outside the instrument to avoid any disturbance due to heat generated in the motor. For the same reason the motor is mounted on perspex pillars to minimize conduction of heat to the rest of the instrument.

Fig. 26. is a close-up of the guiding microscope and the scanning diaphragm. The aperture in the latter is too small to be seen in the photograph.

Transmission curves of the filters to be used with the instrument are shown in figs. 18 and 19. Both filters are of double half wave construction (1-spacer-3-spacer-1), so as to obtain an approximately rectangular pass band. In the case of the short wave filter (8-9μ) the side bands were cut out on the short wave side by the indium antimonide filter, and on the long wave side by the substrate of the filter (CaF_2), which does not transmit beyond 10μ. The long wave filter showed a pronounced side band at 9-10μ, which was reduced to harmless proportions by depositing a reflecting multilayer stack on the reverse side of the filter substrate. Long wave side bands for this filter are cut out by the BaF_2 field lens in the instrument, which absorbs beyond 13μ.

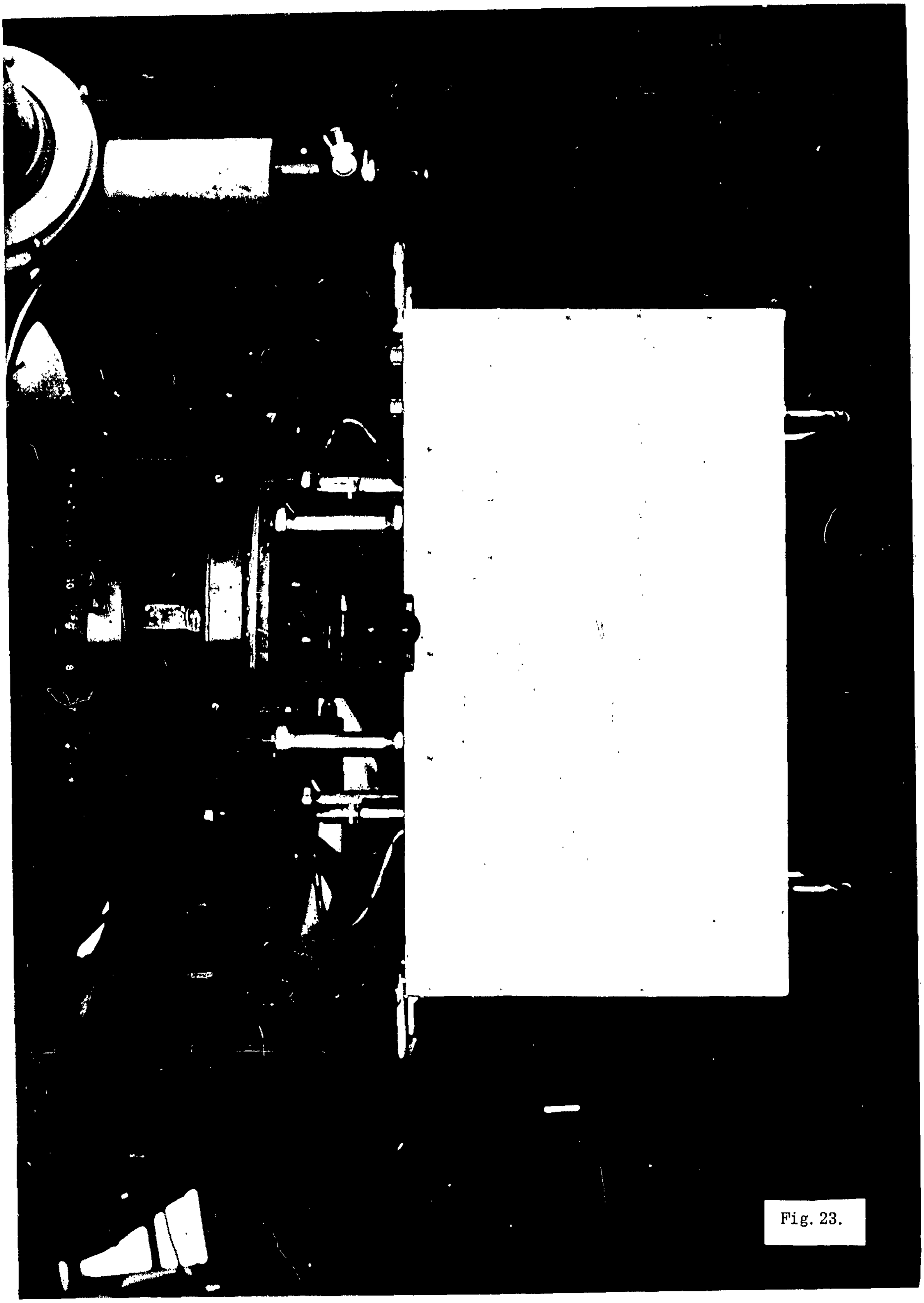

Fig. 23.

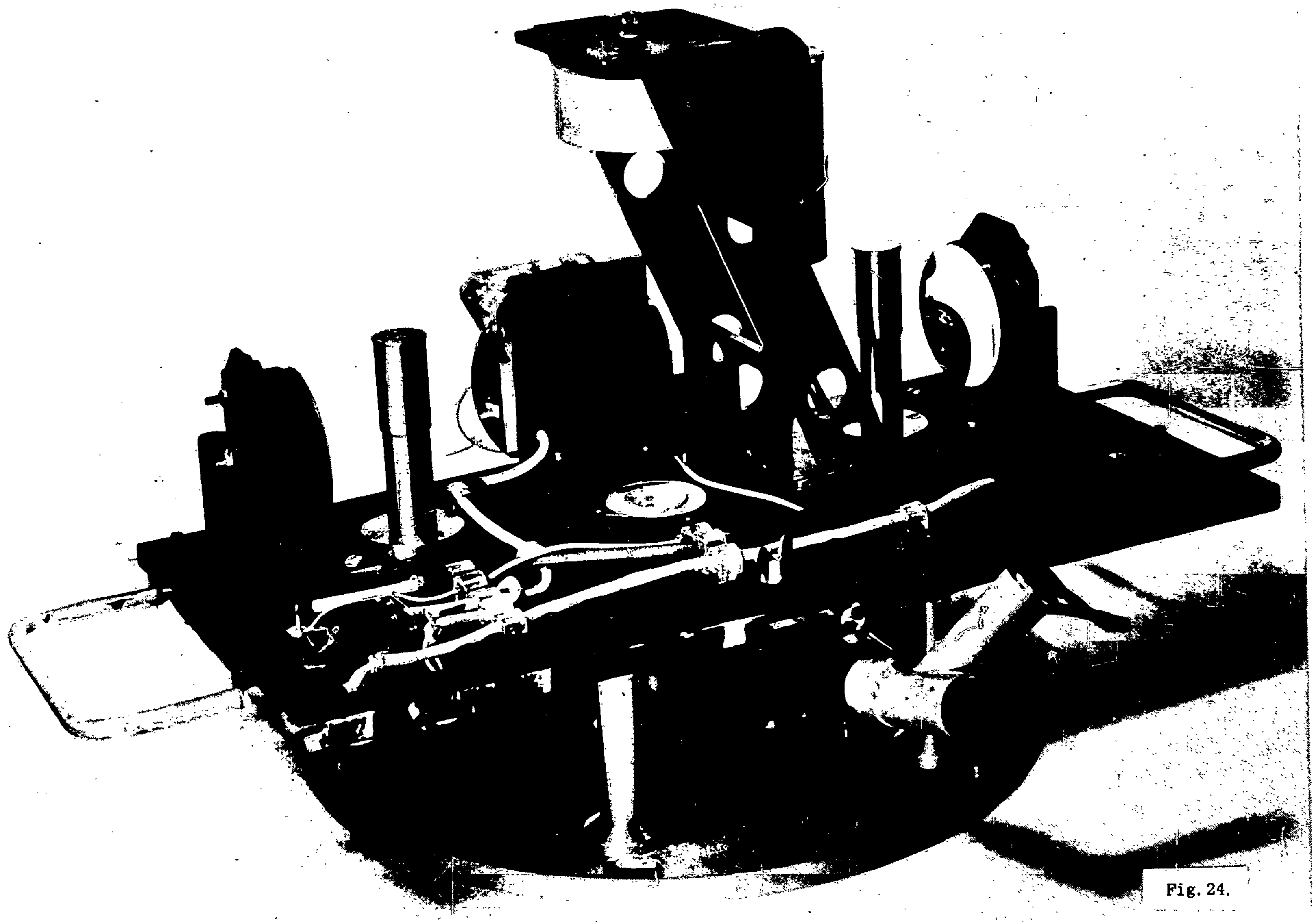

Fig. 24.

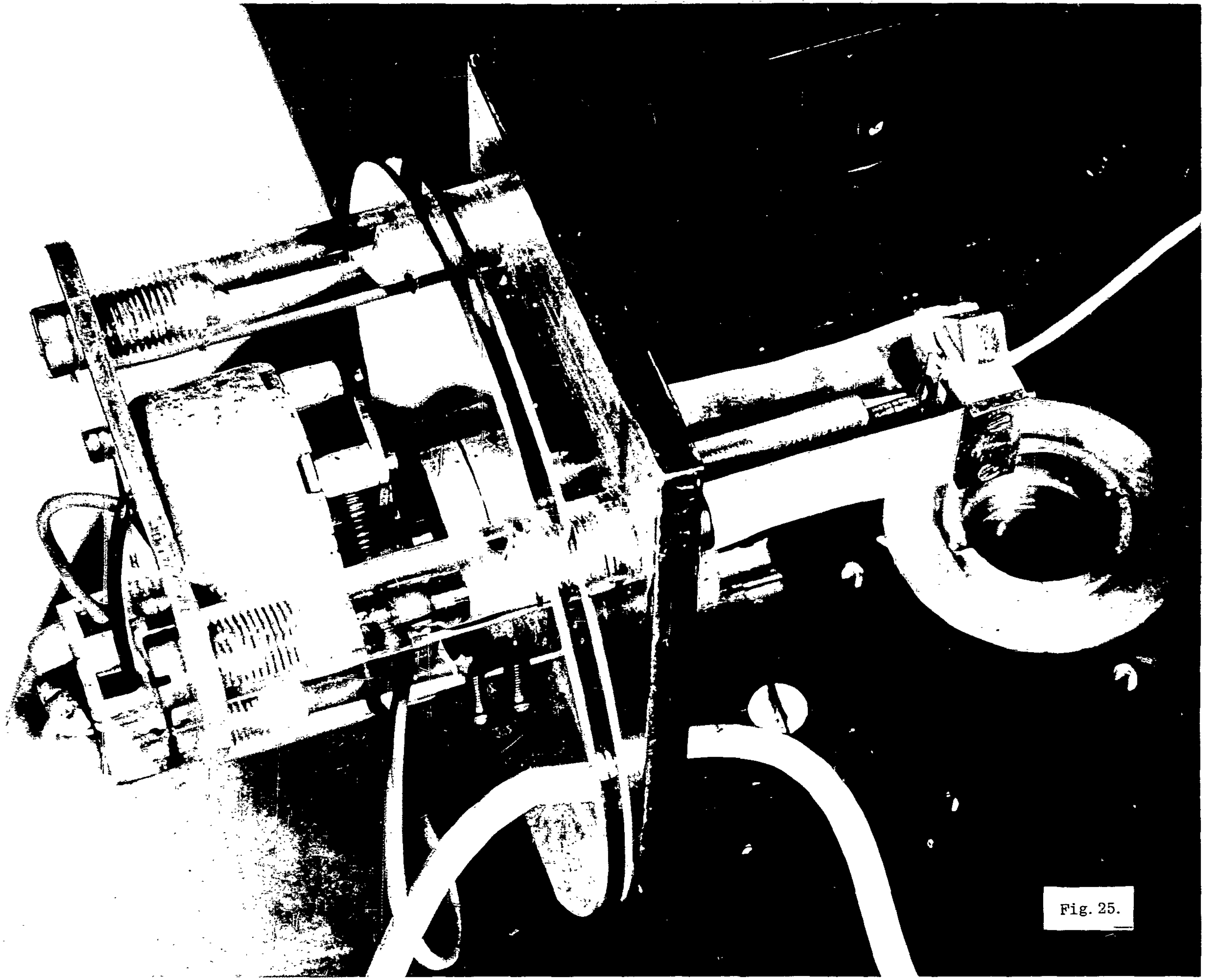

Fig. 25.

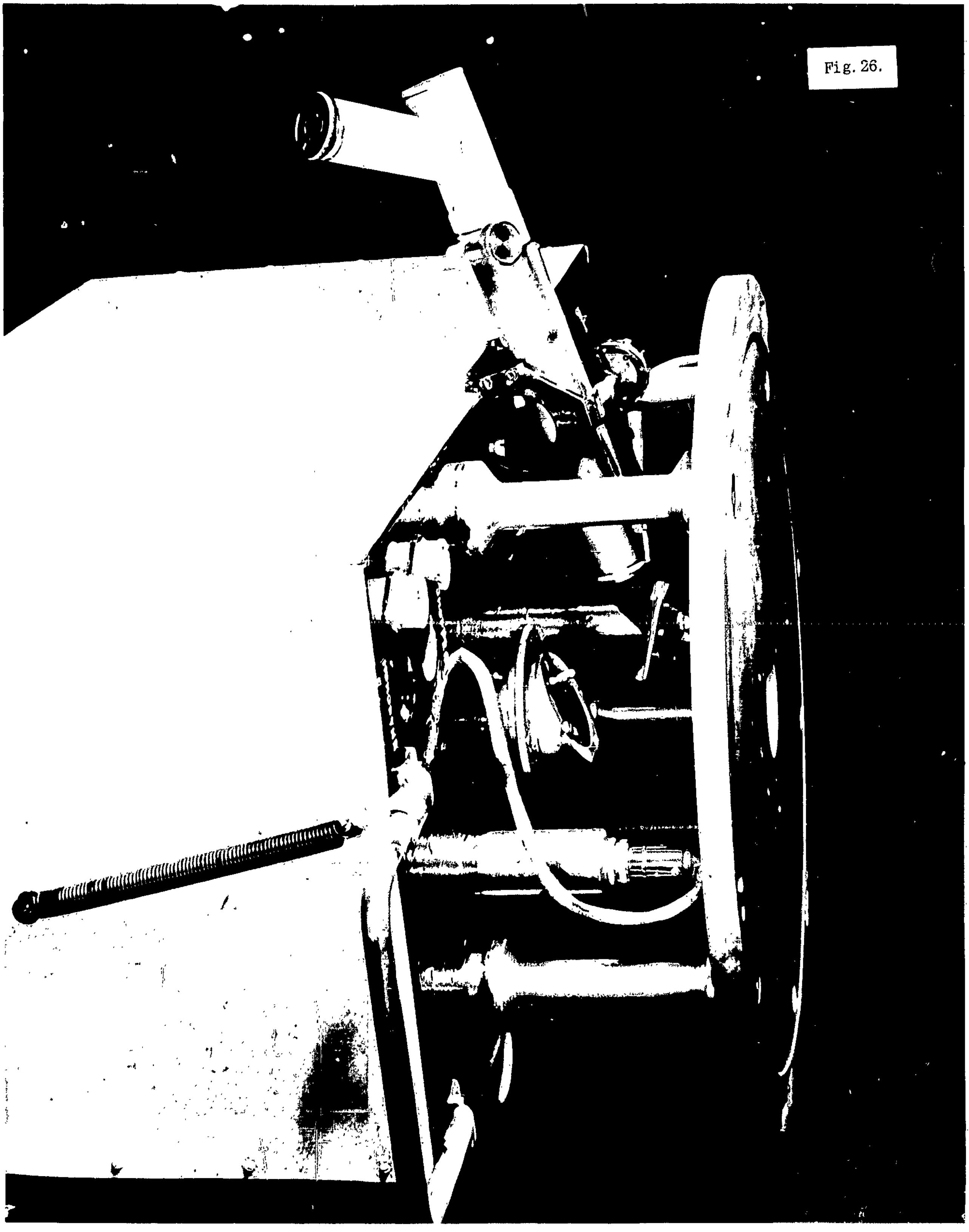

Fig. 26.

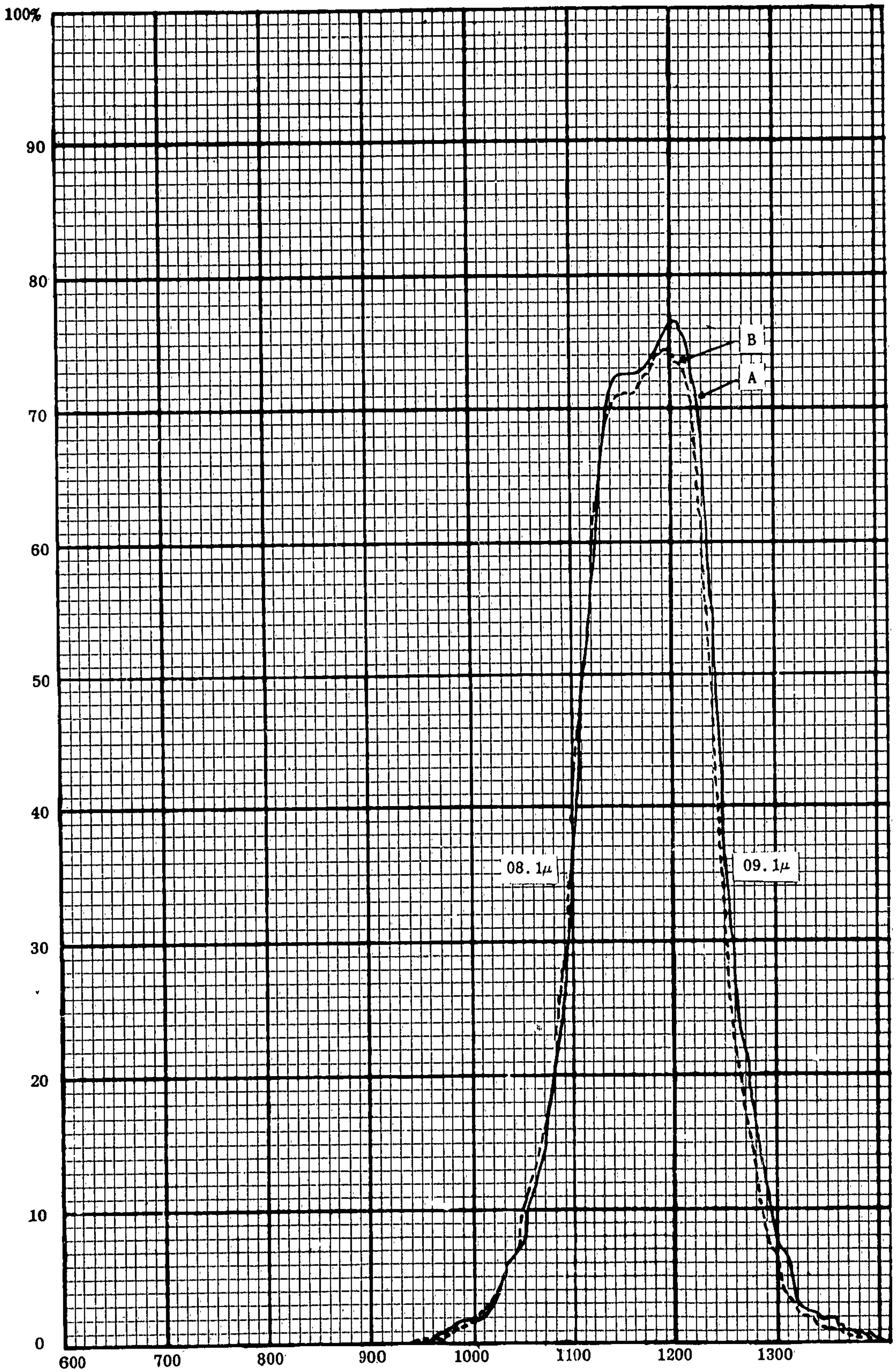

Fig. 18. D.H.W. Filters Controlled on 8.6μ

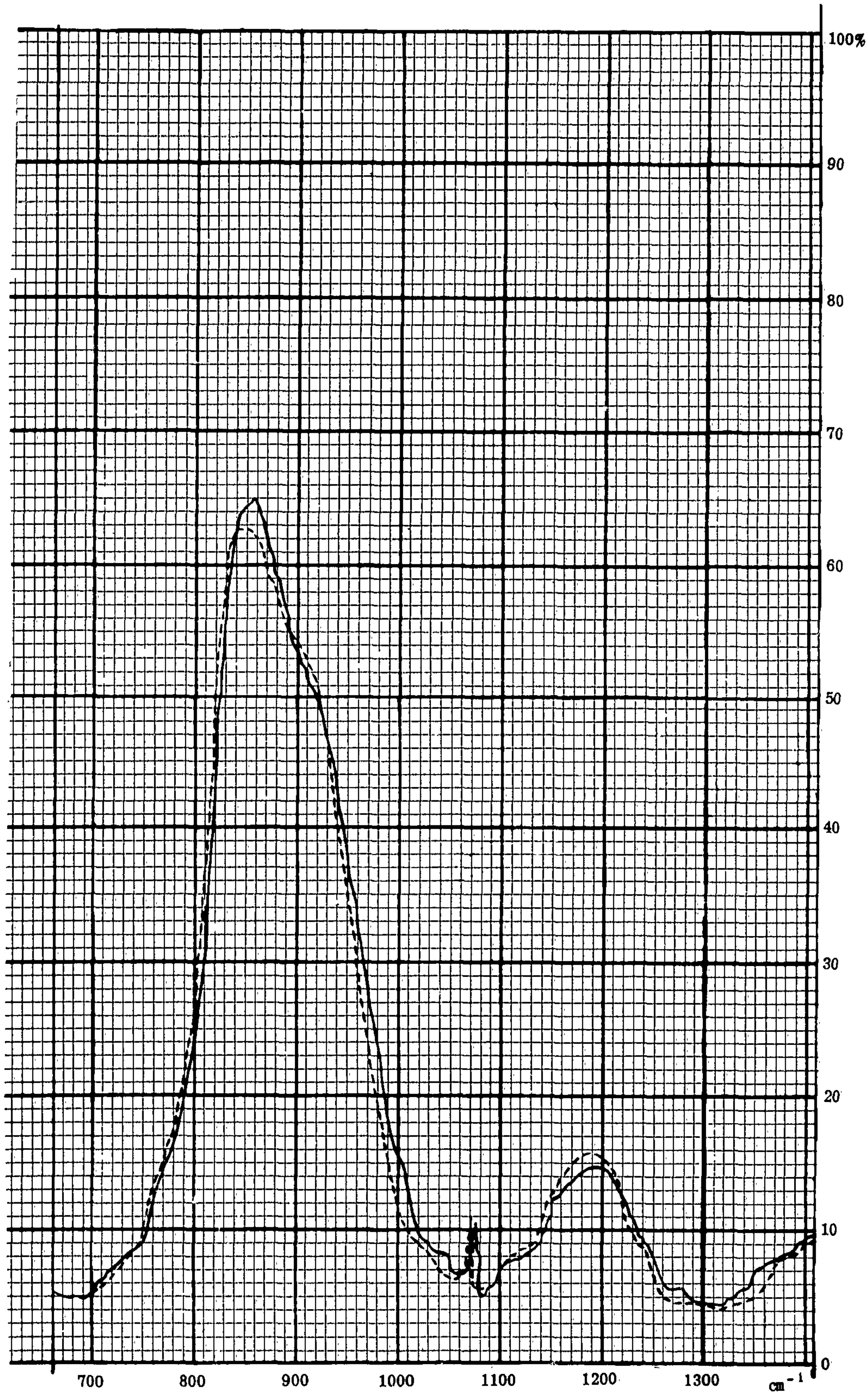

Fig. 19. TRANSMISSION

Laboratory tests of instrument

During development testing of the instrument a considerable number of modifications were found necessary. These concerned mainly the chopping mechanism, which was originally designed as a revolving, sector type chopper. It was found that this chopper itself caused a signal to appear at the output of the thermocouples - possibly due to heat being conducted from the driving motor to the chopper blades. This trouble was eventually overcome with the design of the oscillating prism type chopper, in which the thermocouples always see the same area of the prism, so that even if the prism warms up, no a.c. signal can be generated.

It was found that obviously the instrument was sensitive to changes in the ambient temperature. In fact, after a sudden change of temperature of about 5°C it took about two hours to reach thermal equilibrium at the new temperature. This underlines the necessity - in astronomical use - to keep the instrument in the telescope dome at a temperature close to the outside temperature, so that no sudden change is introduced when opening the dome shutter, This will not present any difficulty in winter, but may amount to quite a problem in summer, when observing nights are short anyhow, and any loss of time to allow the instrument to reach thermal equilibrium would be serious.

It was also found that after changing the scanning diaphragm for one of a different size, or after touching it for some other reason, about 15 minutes have to be allowed before a steady reading is obtained.

Taking adequate precautions it was found that the readings obtained were steady and reproducible within close limits. These limits - in terms of least temperature difference detectable - depend on the actual temperature measured, because for a black body the rate of change of emission with temperature increases with temperature.

Under laboratory conditions it was found that in the range of 40°-80°C, and using a scanning aperture corresponding to 11 seconds of arc on the telescope, temperature differences of less than 1/4° could be detected with certainty.

The thermocouple - being a "black" detector - should show a response proportional to the energy falling on to it, irrespective of the spectral characteristics of the radiation. This was in fact found to be the case, by taking a number of cooling curves between 100° and 0°C, and calculating from Plank's formula the amount of energy radiated at a number of temperatures within the spectral band accepted by the instrument. Departures from proportionality between energy and chart deflection were found to be of the order of the experimental error, and randomly distributed. (See fig. 27).

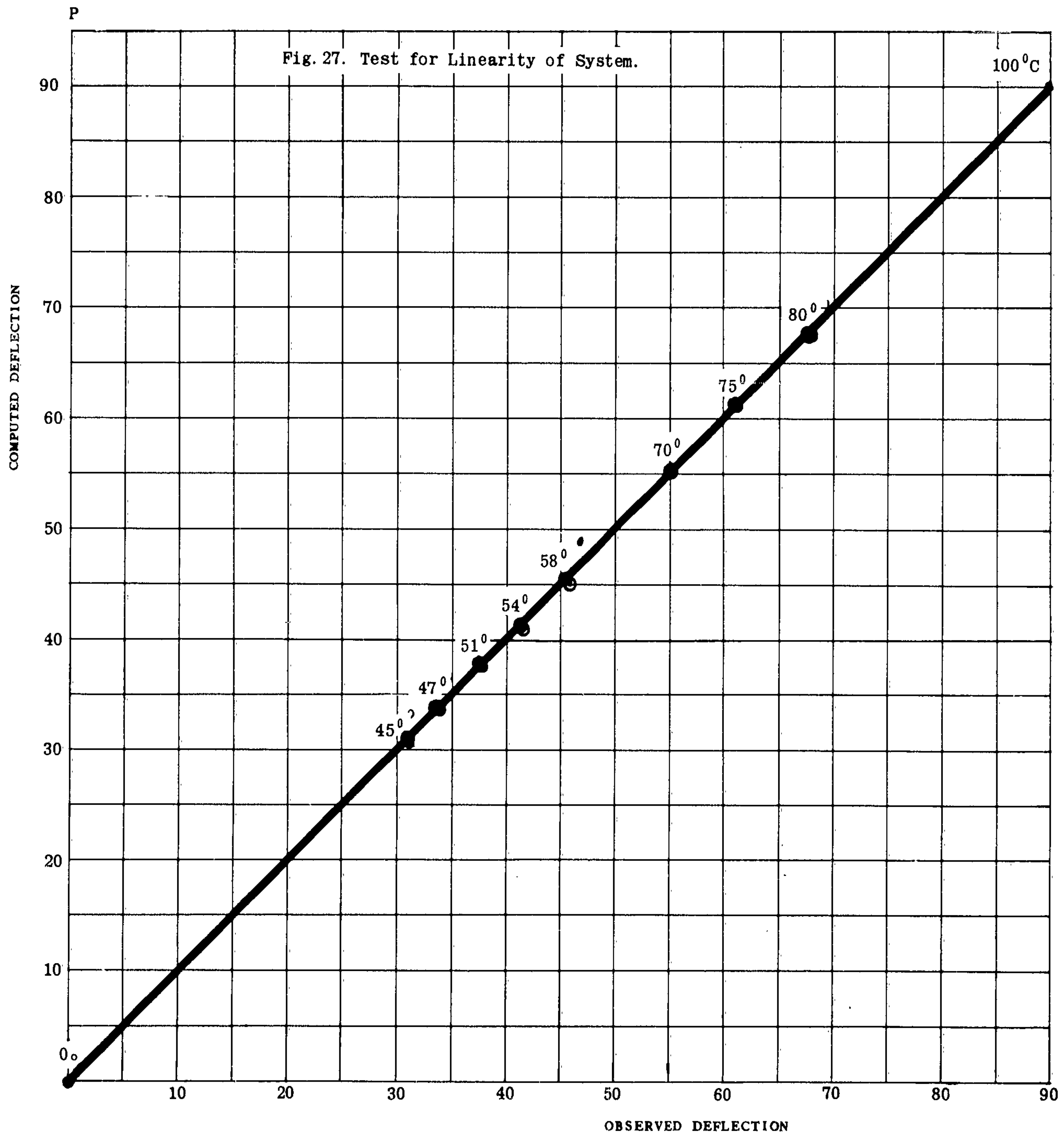
P
Fig. 27. Test for Linearity of System.
100°C
80°
75°
70°
58°
54°
51°
47°
45°
0°
COMPUTED DEFLECTION
OBSERVED DEFLECTION
10
20
30
40
50
60
70
80
90

III. EXPERIMENTAL RESULTS

The following is a summary of results obtained with the instrument described in the previous section in the course of an observing trip to the Osservatorio Astrofisico di Asiago, during December 1961 and January 1962.

Observing periods alloted to the writer during this period are shown in the following table:-

Date	Comments
14/12/61	Cloudy
15/12/61	Variable haze - large noise due to this - results useless.
21/12/61	Good observing conditions until 20.00 U.T. Then dense haze.
22/12/61	Cloudy
28/12/61	Cloudy
29/12/61	Cloudy, relative humidity 100% !
30/12/61	Rain
12/1/62	Broken cloud to start with - completely overcast by 21.00 U.T.
13/1/62	Completely overcast
14/1/62	Dense haze
15/1/62	Good night - 6 hours observations
20/1/62	Full moon - slight variable haze - intermittent scans possible - observations on and off for 10 hours
21/1/62	Heavy haze
22/1/62	Unbroken cloud
26/1/62	Cloudy until 15.00 U.T. - then clear, but extremely poor seeing - scintillation approximately 5″ - impossible to guide on small features.
27/1/62	Dense haze

It is evident from the foregoing table that weather conditions were extremely unfavourable - out of 16 nights useful observations could be obtained during part of 3 nights only. Furthermore, during the whole period the relative humidity never dropped below 70%, and on most nights was around 90%. This fact, apart from reducing the atmospheric transparency in the infra-red, caused the filters for the long wave region to deteriorate, (hygroscopic materials had to be used in the construction of these filters), and in fact, after the first observing session (21/12/61) these filters were no longer used. The techniques described in Section II for the protection of hygroscopic filters will remove this difficulty in future observations.

a) Emissivity measurements

The basis of these measurements is the fact that for a black body the ratio of the energies emitted in two spectral bands is a function of the temperature of the body only. Conversely, knowing the ratio of the two energies, the temperature can be determined. If the body is not a black body, i.e. if the emissivity is less than unity, then, providing that the emissivity is substantially the same in the two spectral bands, this ratio remains unchanged, and still provides a measure of the temperature.

Thus if:-

E_1 and E_2	are the energies *radiated* by the moon in the bands $\lambda_1 - \lambda_2$ and $\lambda_3 - \lambda_4$
H_1 and H_2	are the engeries *received* in the same bands
τ_1 and τ_2	are the atmospheric transmissions in the two bands
ϵ	is the emissivity of the moon's surface (assumed constant over the range $\lambda_1 - \lambda_4$)
$F(T, \lambda)$	is Planck's black body function

Then:-

$$E_1 = \frac{1}{\tau_1} H_1 = \epsilon \int_{\lambda_1}^{\lambda_2} F(T_1 \lambda)\, d\lambda$$

$$E_2 = \frac{1}{\tau_2} H_2 = \epsilon \int_{\lambda_3}^{\lambda_4} F(T_1 \lambda)\, d\lambda \qquad (1)$$

H_1 and H_2 are quantities determined by measurements. If in addition τ_1 and τ_2 are known, then from the ratio of the energies T can be determined, without any knowledge of the emissivity ϵ. Knowing T, either of the equations (1) will give a value for the emissivity ϵ.

It is evident that the success of the experiment is dependent on the knowledge of the quantities τ_1 and τ_2, the atmospheric transmissions in the two wavelength regions. The only way of obtaining values for these quantities (short of high-altitude balloon or satellite experiments) is by measuring the extinction of the moon as a function of zenith distance and extrapolating to zero air mass.

As the atmospheric transparency in the spectral regions considered varies appreciably with the water vapour content of the air, these measurements of extinction must be made on the same night as the measurements of radiant energy. Furthermore, as the extinction measurements will occupy a period of some hours during which the temperature of most areas of the moon will undergo an appreciable change, the measurements should be made in the area of the subsolar point, and preferably at or near full Moon, under which conditions this temperature variation is smallest.

Unfortunately, during none of the three nights in which observations were possible was there a sufficiently long period of clear and constant weather conditions to enable the experiment to be performed successfully. This part of the programme will therefore have to be repeated at some future opportunity.

b) Temperature "anomalies"

The second part of the programme consisted of a search for temperature anomalies, i.e. local differences of temperature which could not be ascribed to differences in insolation. This search was prompted by Sinton's discovery of the anomalous behaviour of the crater Tycho as compared with its surroundings, during a lunar eclipse [10], and ascribed by him to different thicknesses of dust covering the crater floor and the regions surrounding the crater.

As Tycho is the most prominent crater of the class known as "ray craters", this survey was directed at other members of this class.

Anomalies were observed in the following craters:-

1) Proclus

2) Manilius

3) Copernicus

None of the other craters examined so far, including Tycho, Aristarchus and Kepler showed any noteworthy anomalies. Due to lack of time the survey was by no means complete, and many other craters and other features remain to be observed.

The craters were examined by recording the energy flux from the crater itself (in all cases the scanning aperture was chosen so as to be not larger than the crater itself; mostly aperture No. 2 - 11″ diameter). By using the telescope motions in right ascension and declination, four points were recorded, which were displaced from the crater centre in four directions at right angles to each other, denoted by "north, south, east, west". East and west were labelled to agree with the cartographic (not astronomical) nomenclature. No filters were used, because temperature differences only were looked for, and using the whole spectral band which the instrument could accept, maximum sensitivity could be obtained.

In each of the three anomalous cases referred to above it was found that the crater centre was cooler than the four surrounding areas. Tracings of the chart recordings obtained are shown in fig. 28, 29 and 30, and it is evident that the effect is large compared with instrumental noise. The latter is mainly due to guiding inaccuracies.

To find approximate values for the temperature of these points, a reasonable value has to be assumed for the atmospheric absorption. In the present case this has been taken as 15%. This figure is of course quite arbitrary, and changing it will give a different value to the temperature. Assuming this atmospheric transmission it is possible to convert the recorded deflections into temperatures, using as calibration points the readings of the 100^0C black body and of ambient temperature, both of which were recorded at frequent intervals during each observing session, and were found to remain steady over periods of several hours. This conversion into temperatures was done graphically, as shown in figs. 31, 32 and 33 for the three craters.

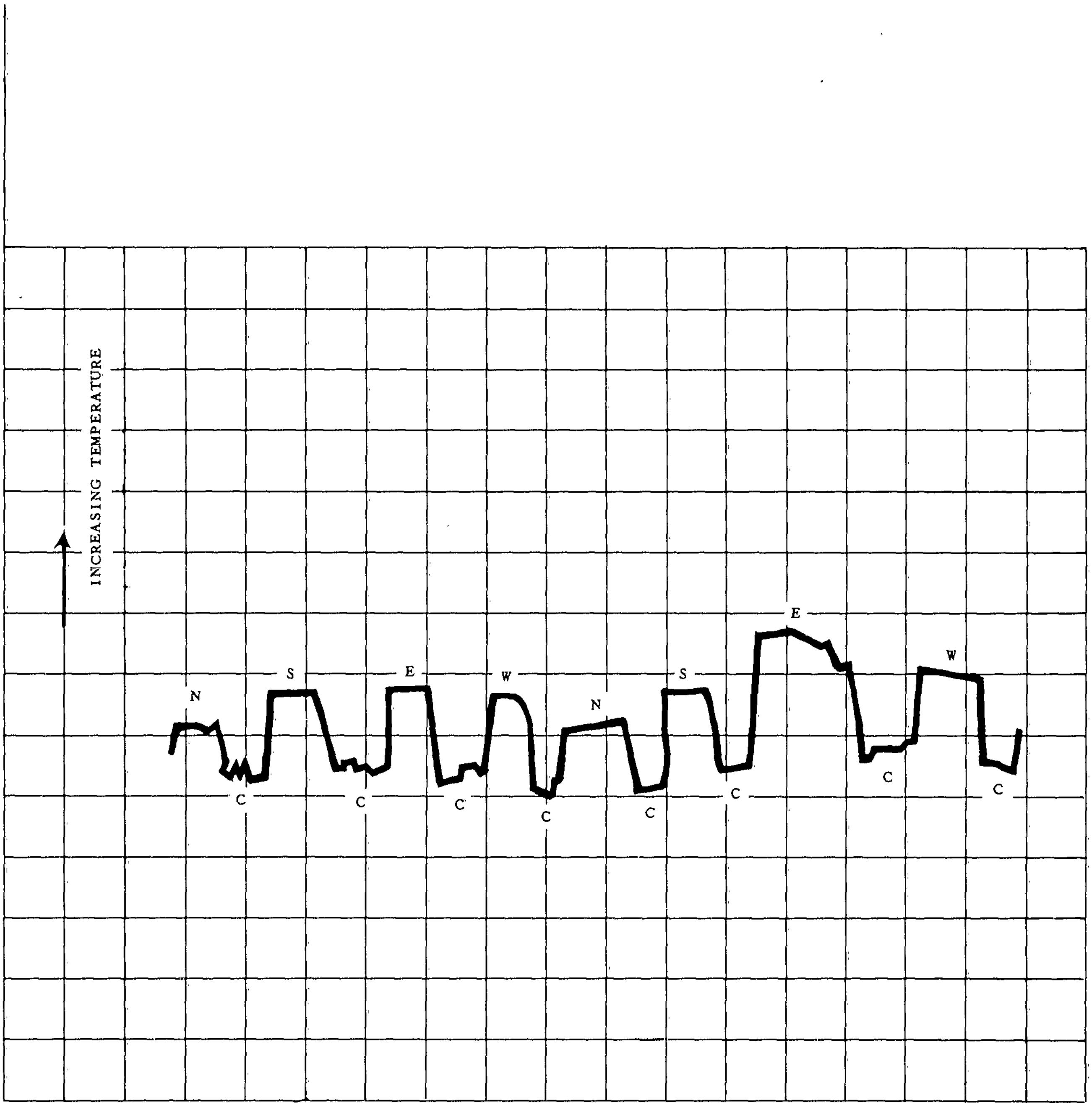

Fig. 28. Tracing of Chart Record of Temperatures of Environs of Proclus.

C - CRATER CENTRE
N - 1 CRATER DIAMETER NORTH OF CENTRE
S - 1 CRATER DIAMETER SOUTH OF CENTRE
E - 1 CRATER DIAMETER EAST OF CENTRE
W - 1 CRATER DIAMETER WEST OF CENTRE .

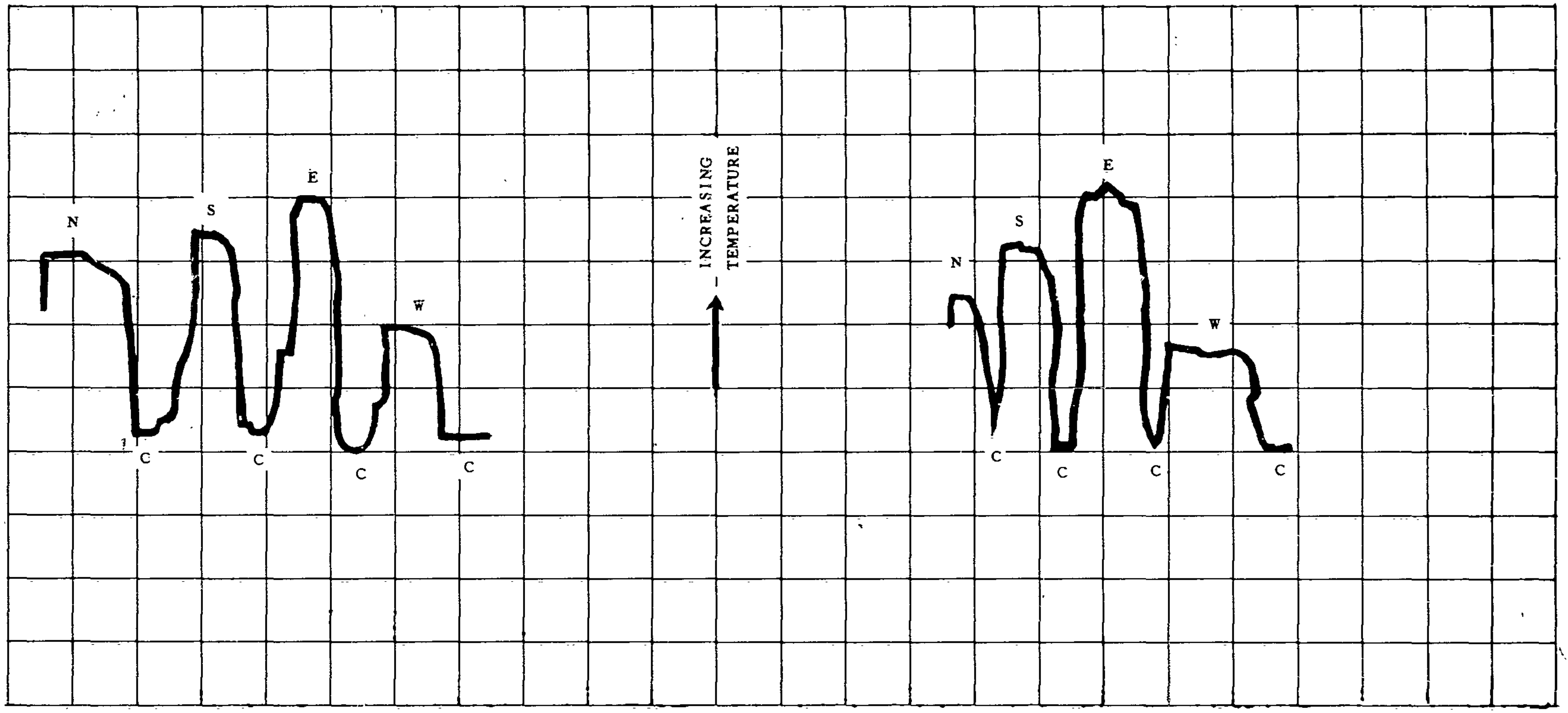

Fig. 29. Tracing of Chart Record of Temperatures of Environs of Manilius.

C - CRATER CENTRE
N - 1 CRATER DIAMETER NORTH OF CENTRE
S - 1 CRATER DIAMETER SOUTH OF CENTRE
E - 1 CRATER DIAMETER EAST OF CENTRE
W - 1 CRATER DIAMETER WEST OF CENTRE

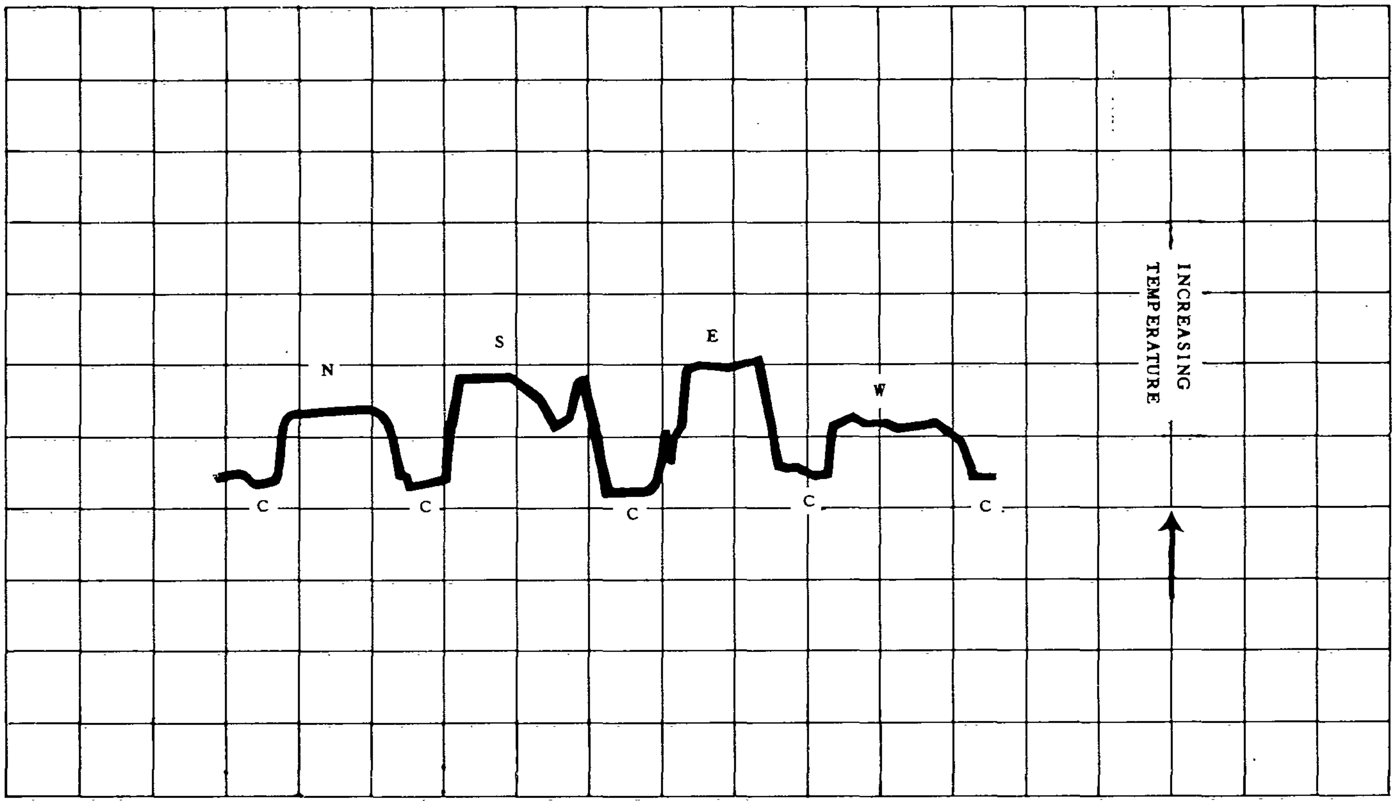

Fig. 30. Tracing of Chart Record of Temperatures of Environs of Copernicus.

C - CRATER CENTRE
N - 30″ NORTH OF CENTRE
S - 30″ SOUTH OF CENTRE
E - 30″ EAST OF CENTRE
W - 30″ WEST OF CENTRE

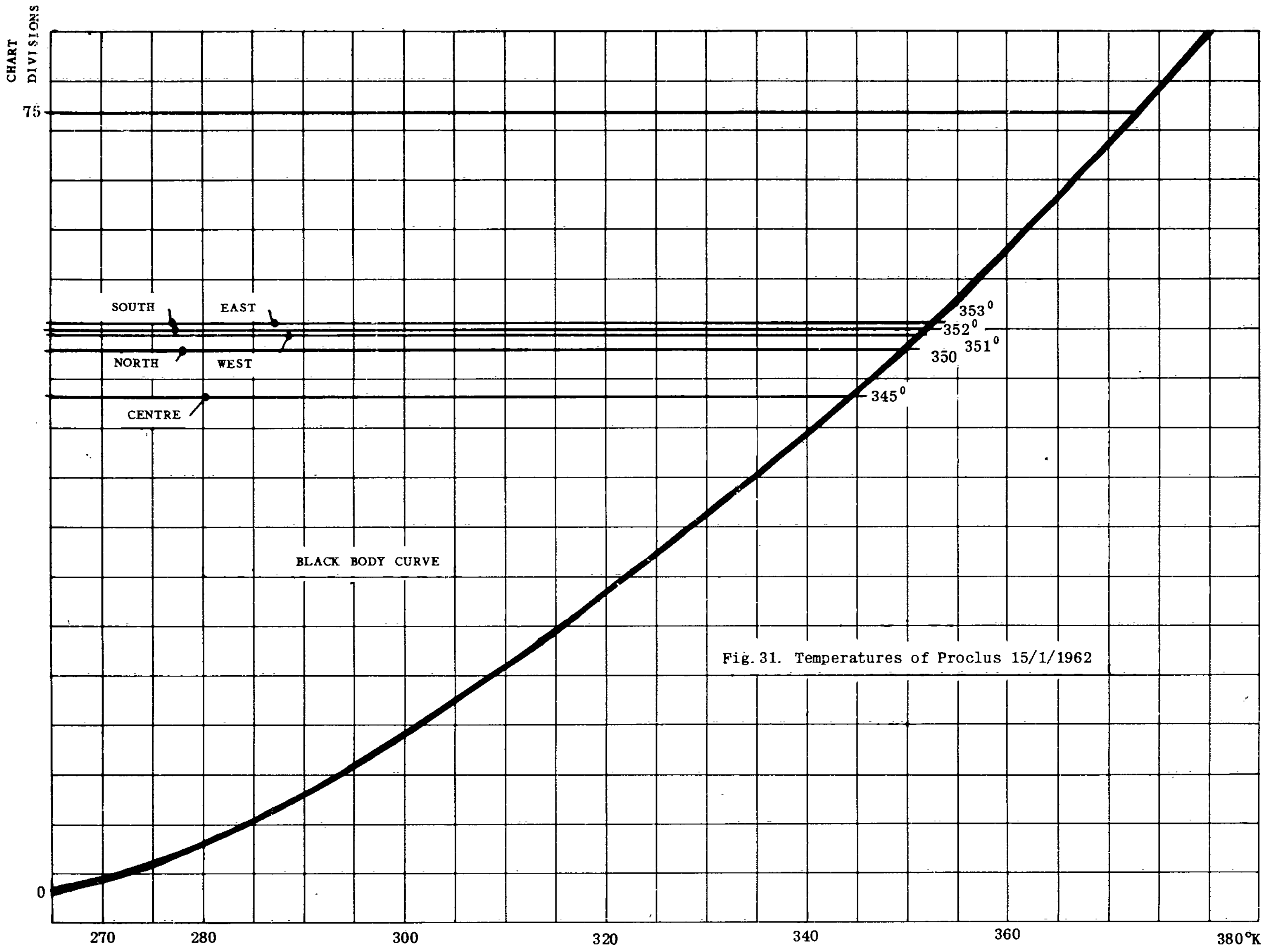

Fig. 31. Temperatures of Proclus 15/1/1962

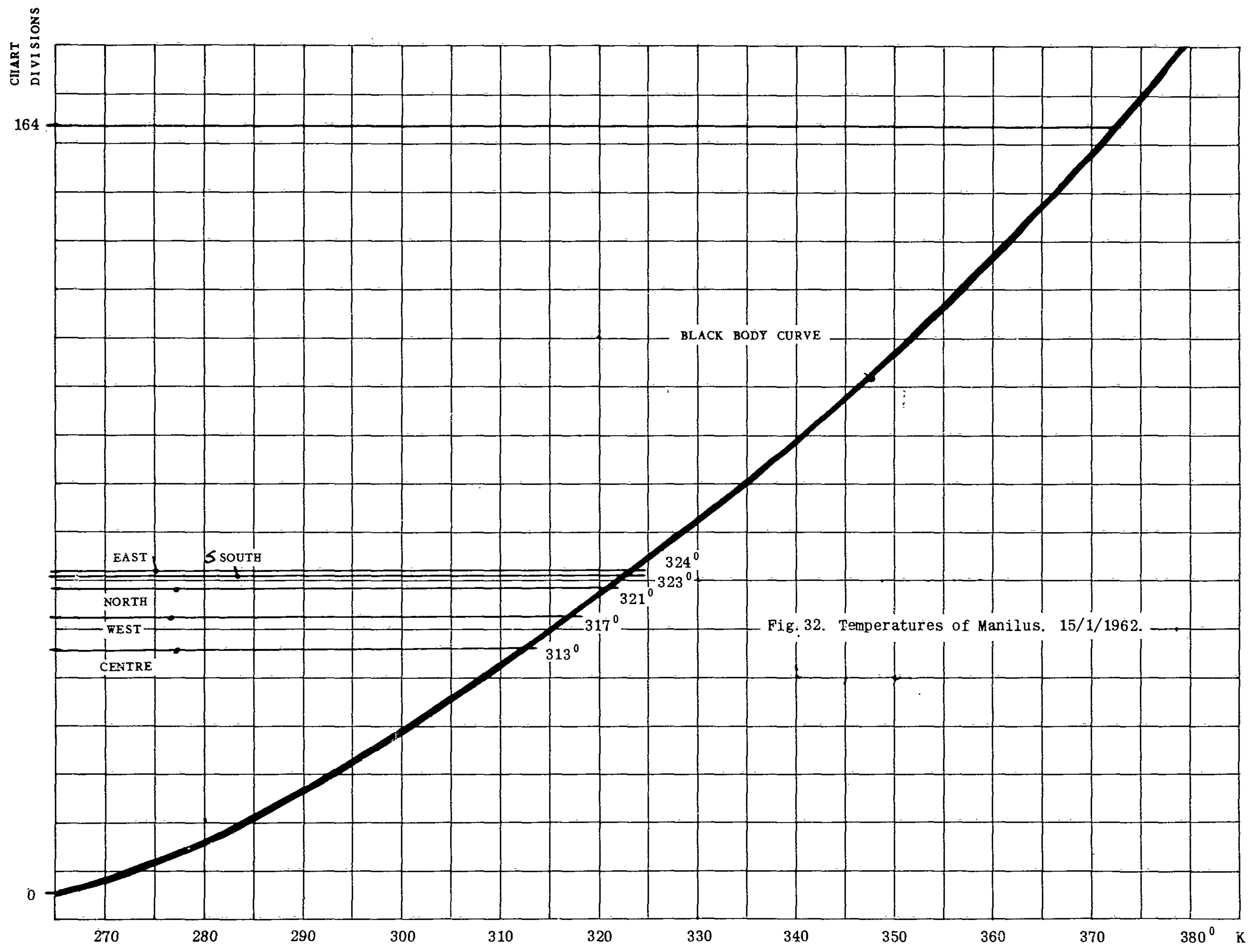

Fig. 32. Temperatures of Manilus. 15/1/1962.

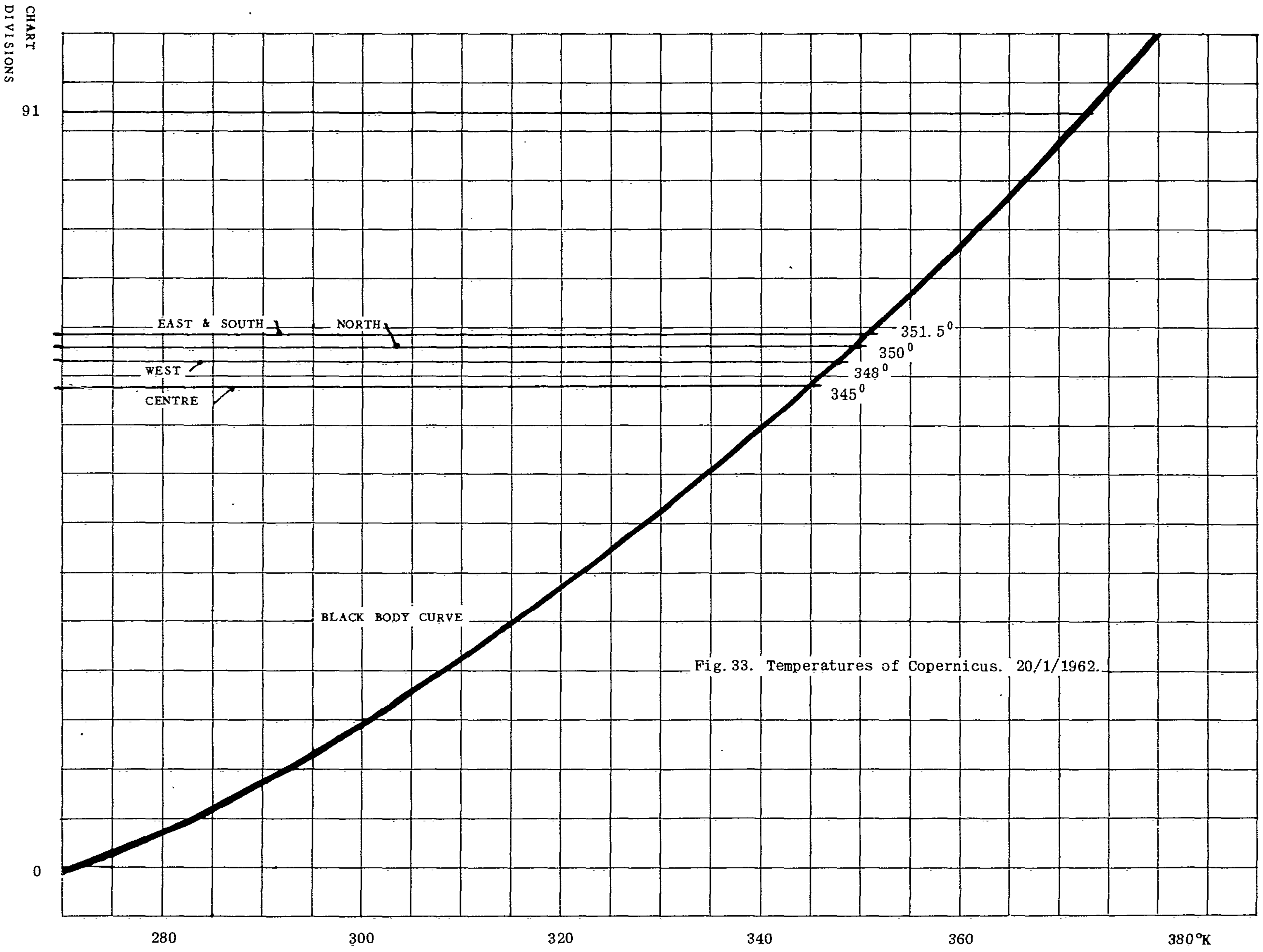

Fig. 33. Temperatures of Copernicus. 20/1/1962.

As mentioned these temperatures are uncertain because of the lack of knowledge of atmospheric transmissions. However, as the change of slope of the black body curve in the regions concerned is small, the temperature *differences* between the different points will be little affected by this factor. From the slope of the curve it is possible to find the temperature difference corresponding to one chart division, and so obtain reliable values for these differences. Temperature differences relative to the crater centre are shown diagrammatically in fig. 34. The general temperature gradient in the direction of the sub-solar point is evident in all diagrams. The values of the temperature differences are considered reliable to $\pm \frac{1}{2}^0$.

As to the reasons for these anomalous temperature differences no definite conclusions can be drawn on the basis of the presently available data. Fig. 34 shows that the temperature anomalies persist at different altitudes of the sun with respect to the moon - data having been obtained on the 15/1/1962 and on the 20/1/1962, i.e. 2 days after first quarter and at full Moon. The temperature differences are naturally modified by the different general temperature gradients on the two dates.

Two possible explanations of the effect are the following:-

1) The thermal conductivity of the surface material in the crater is higher than that in the regions surrounding the crater. This explanation would be in agreement with the hypothesis that ray craters are impact craters of fairly recent origin (astronomically speaking), so that it could be surmised that the material in the crater centre has been compacted by the impact, and loose rubble or dust has been scattered over the surrounding areas.

2) The surface albedo in the visible and near infra-red regions (near the maximum of the solar energy spectrum) is higher in the crater centre than in the surroundings, so that less heat is absorbed in the centre.

If the first hypothesis is correct, then during the lunar night the temperature anomaly should be reversed, because heat would be more readily conducted from the constant temperature interior of the Moon in regions of high conductivity; hence the crater centre should be warmer.

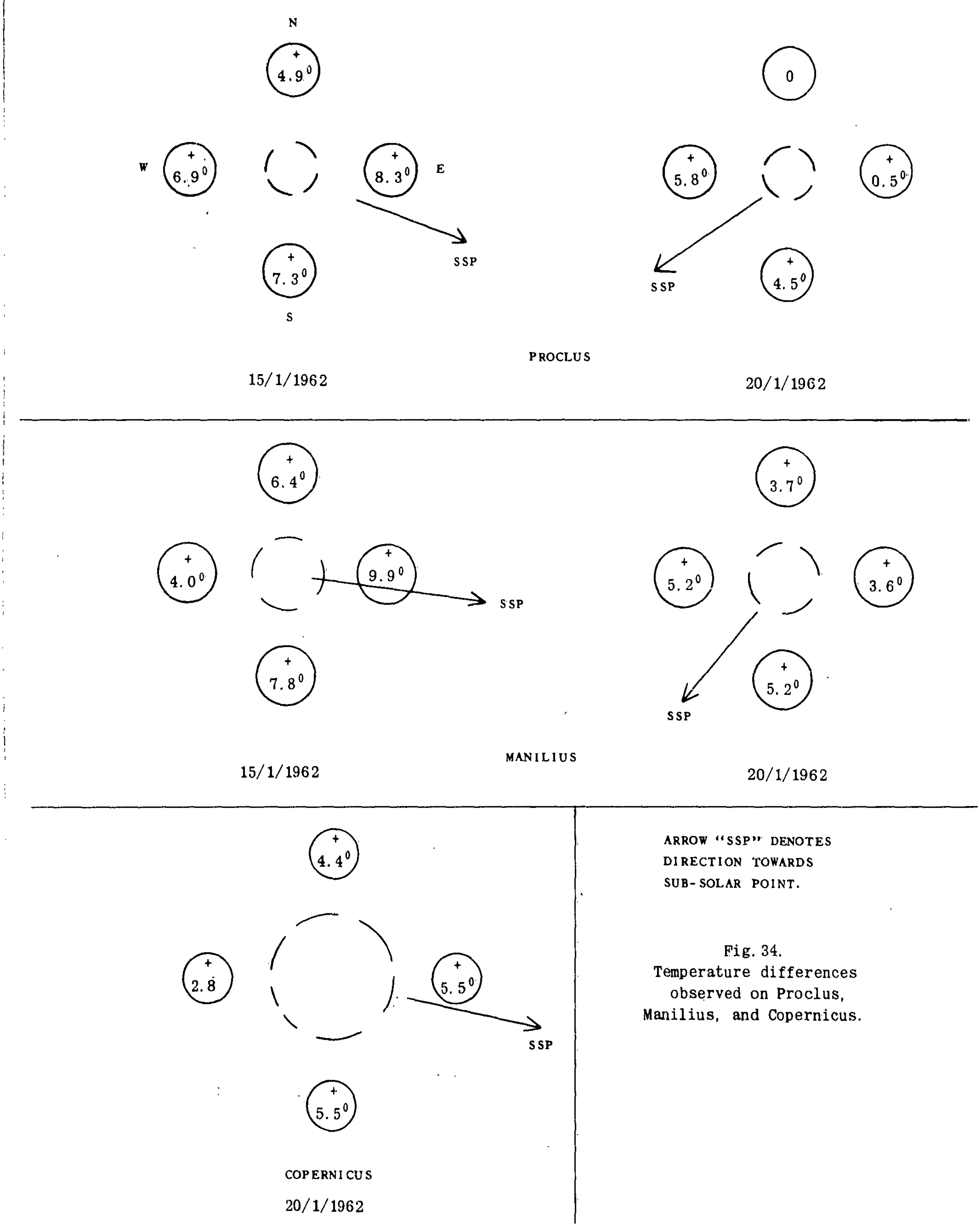

Fig. 34.
Temperature differences observed on Proclus, Manilius, and Copernicus.

If the second explanation is the correct one, then:-

(a) the anomaly should disappear during the lunar night;

(b) there should be a correlation between densitometer readings in a photograph of the crater area, and observed temperatures, inasmuch as areas of high albedo (showing high density on a photographic negative) should appear to be cooler.

Point (b) above was tested by making microdensitometer tracings across Proclus and Manilius on a negative taken at the Pic-du-Midi Observatory on the 20/1/1962 (full moon). These tracings are shown in figs. 35, 36, 37 and 38 and indicate for both craters a lower density for the crater centre relative to the surrounding areas. This is exactly opposite to what would be expected according to hypothesis 2, and appears to rule out this explanation.

Further, and more detailed observations are required to decide the issue unequivocally.

Planned modifications of instrument

While on the whole the instrument performed satisfactorily, a number of modifications, which could not easily be foreseen during laboratory testing, were found to be desirable to increase operating efficiency and convenience.

(1) Filters:-

At average relative humidities (~50%) in the laboratory the filters were found to be quite stable. Due to exceptionally high humidity during the observing expedition however they became useless after the first night's observations. Hence, in future, filters should be sealed into their mounts with a cover disc of substrate material so as to exclude atmospheric influences. For the long wave filters BaF_2 substrates should be used instead of the NaCl substrates used hitherto. The plug-in arrangement for changing filters was found to be distinctly inconvenient due to the awkward angle of the instrument when mounted on the telescope. Filters should be mounted permanently in a slide or revolving disc, which can be moved from the operator's position.

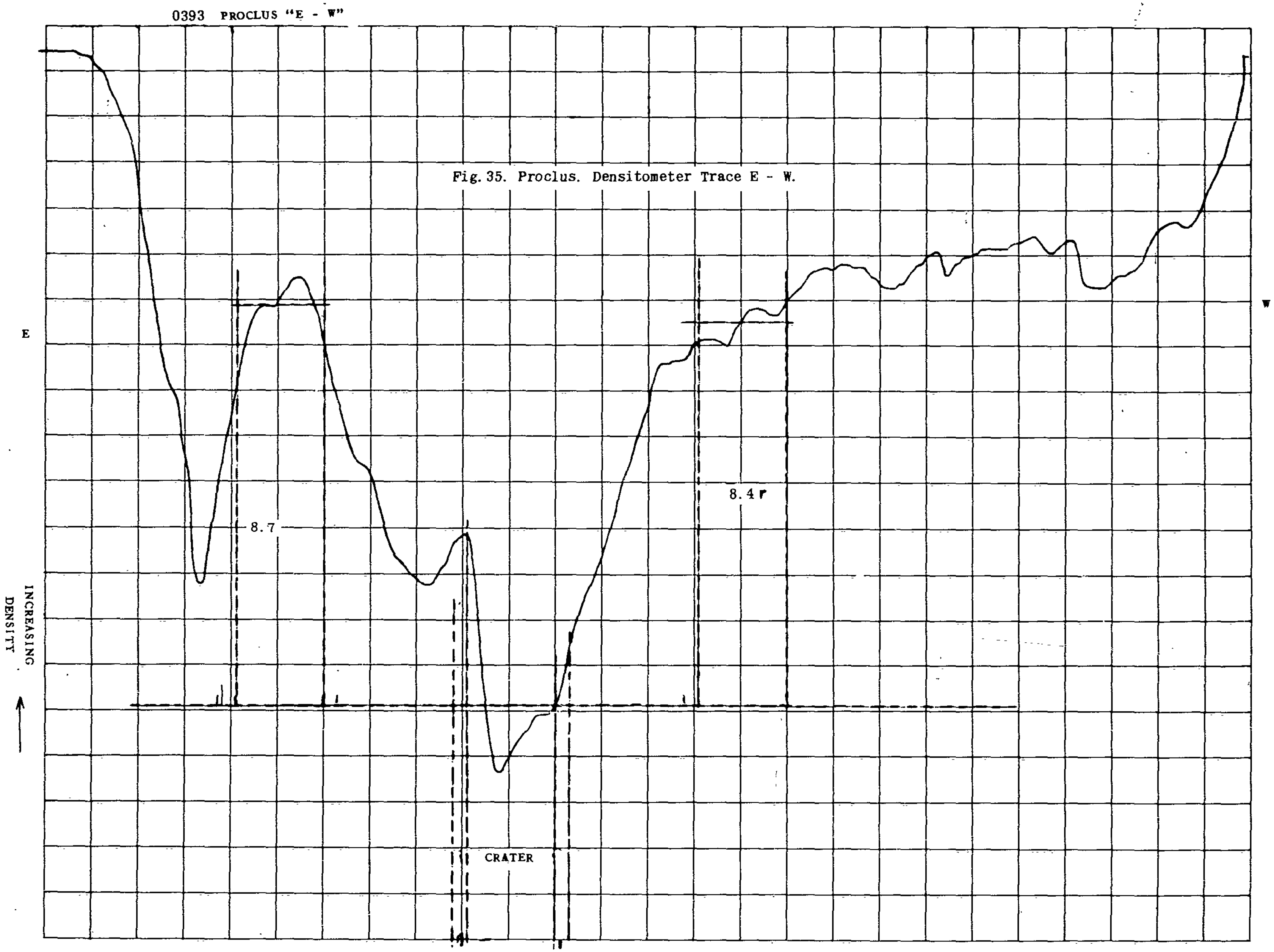

Fig. 35. Proclus. Densitometer Trace E - W.

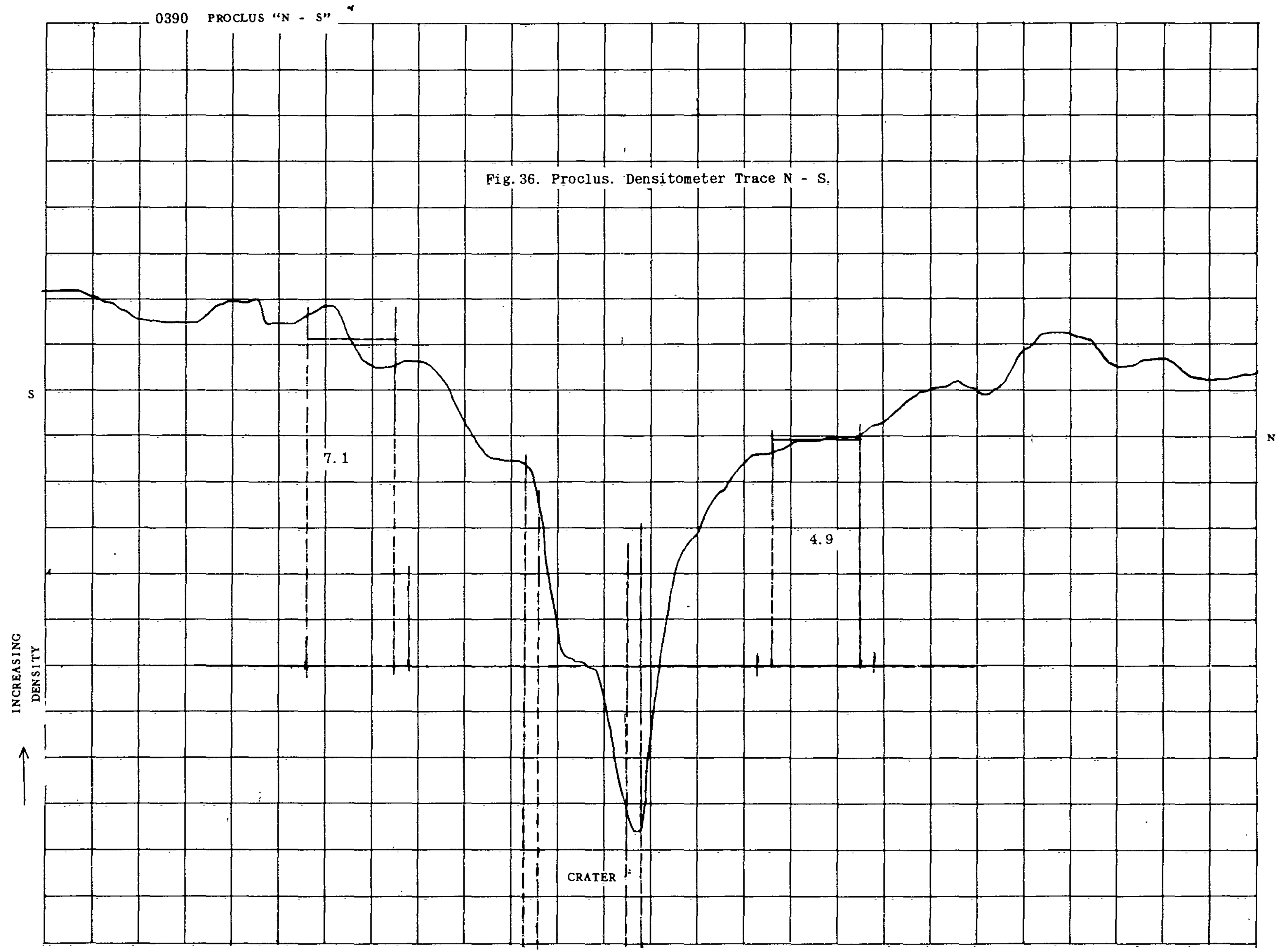

Fig. 36. Proclus. Densitometer Trace N - S.

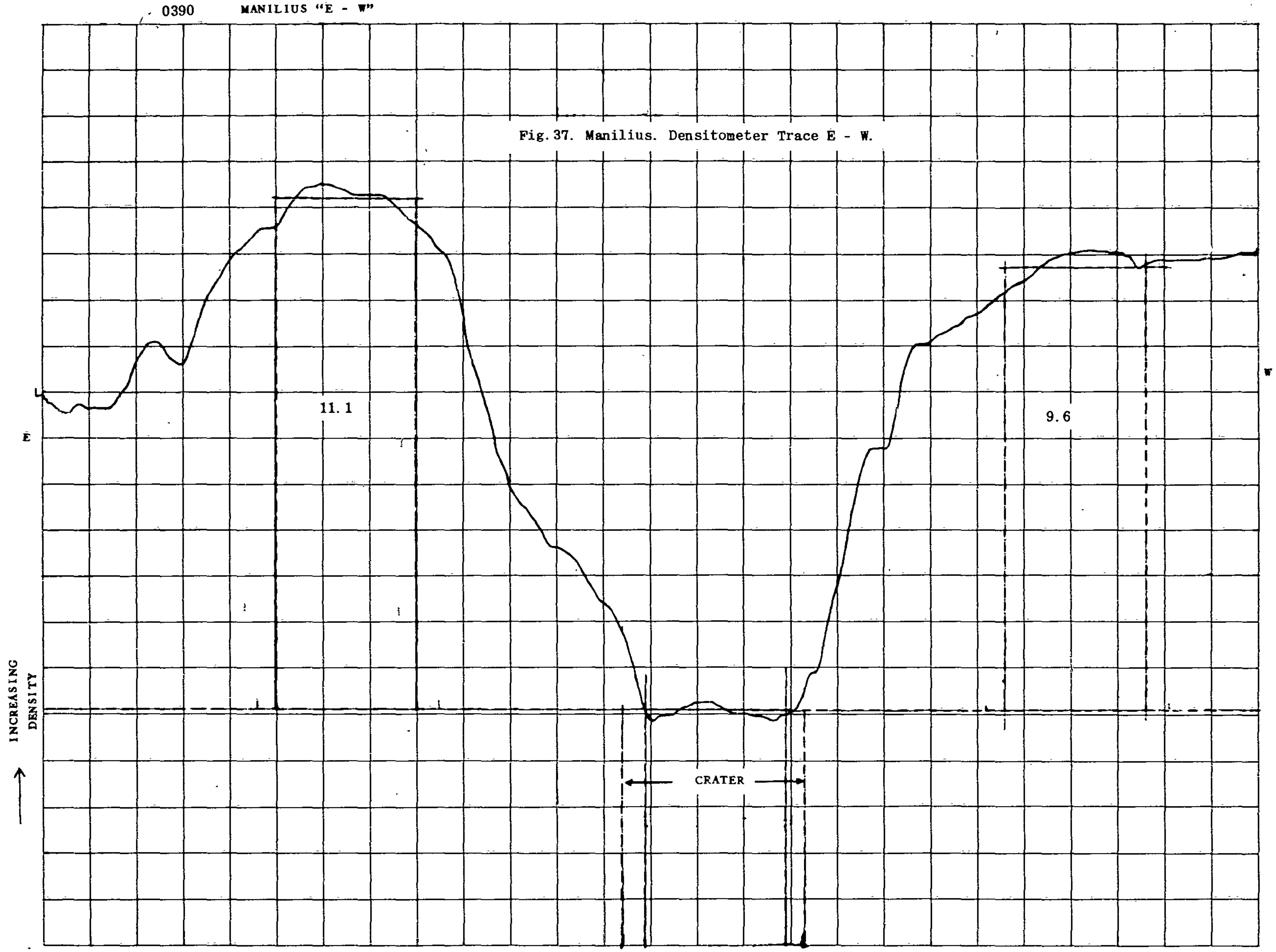

Fig. 37. Manilius. Densitometer Trace E - W.

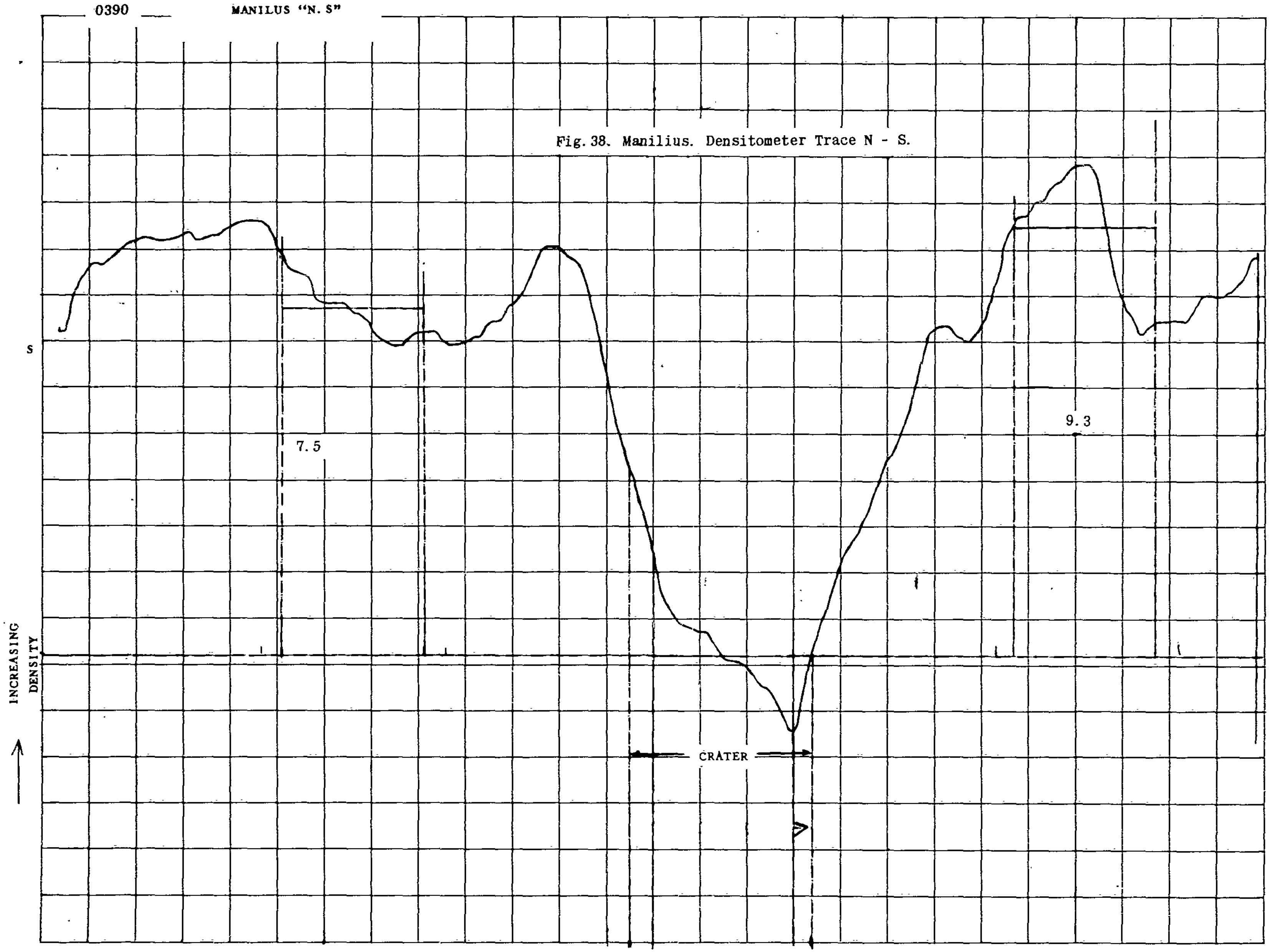

Fig. 38. Manilius. Densitometer Trace N - S.

(2) Guiding arrangements:-

It was found that the combination of high magnification and small field of view of the guiding microscope made it very difficult to guide on low contrast features away from the lunar terminator, where most observations were made.

As regards the magnification this cannot be reduced by a large amount without having the image of the Newtonian flat in the exit pupil so large as to obstruct most or all of the light. It will however be very desirable to increase the field of view by using a specially designed wide angle eyepiece which should give a apparent field of view of about 60^0, instead of the 25^0 of the presently used Huyghenian eyepiece.

Furthermore, it will be desirable to provide means for scanning the image of a crater or other feature in any direction, independently of the telescope guiding motions. The telescope has two speeds of movement in both right ascension and declination, one of which is much too fast, and the other much too slow to be of any use. This scanning movement could for instance be effected by means of a plane-parallel, transparent plate between the telescope and the instrument, which can be tilted so as to displace the image at a controlled rate, the tilting axis being adjustable so that scans can be taken in any direction, instead of right ascension and declination only. The arrangement would be somewhat similar to that in the Markovitz camera.

Some arrangement of this kind will be essential if observations are to be made on features on the dark side of the moon. As the feature to be observed cannot be seen the telescope must be set onto some part of the illuminated hemisphere, and the image then displaced by a known amount in a known direction, as determined from lunar maps.

(3) Black bodies:-

The reference black bodies, as constructed, were found to be too small, inasmuch as one filling of solid CO_2/acetone, or of boiling water did not last very long, and refilling was needed several times during each observing session - a rather time-wasting procedure. Also, the heater spiral in the boiling water black body was made from uninsulated nichrome wire, fed from the mains via a

Variac transformer, as no low tension supply was available on the Newtonian platform. The Variac being an autotransformer meant that the black body was "live", and considerable care had to be exercised in handling it on the metal platform. If a larger black body is made it should be possible to use mineral insulated resistance cable (Pyrotenax), and so avoid this element of risk. If the heater input can be controlled thermostatically to keep the water temperature at, say, 95^{0}C, the danger of boiling dry and the need for refilling will be obviated.

(4) Electronics:-

In general it was found that there was too much electric and electronic equipment on the Newtonian platform for the observer to attend to efficiently, as well as guiding the telescope, moving the dome and platform, and supervising the functioning of the instrument itself. It also meant that it took about one hour to set up the complete equipment for each observing session.

As it is important that the signal lead from the thermocouples to the amplifier should be kept as short as possible, the first amplifier stage should be separated from the rest of the amplifier and built into the instrument. The signal from this stage will be large enough to be passed by cable to the recorder room at the base of the dome without undue loss or interference pick up. The same (multi-core) cable will also carry the power supplies to the head amplifier, chopping motor, and black body. Thus there will be no electrical cabling between the platform and the telescope, giving the observer some freedom to move without the risk of tripping over wires in the dark.

The time constants provided in the amplifier were·too widely spaced, and in fact the longest time constant (21 seconds) was never used, as it took more than one minute to get a steady recorder deflection. Instead of this a further value should be provided between the 2 and 7 second positions, say of about 4 seconds.

It would be desirable to have some means for biassing the instrumental zero off scale by a known amount, so that the scale can be expanded for observations of small temperature differences. This could be done by replacing the zero set control of the amplifier by a multi-position switch and a suitable resistor network.

The homodyne rectifier caused some trouble, but this was not considered to be serious, as the homodyne had to be used only to find the sign, and not the magnitude of any temperature difference. It would however be desirable to replace the mechanical contacts by an optical arrangement, for instance a sector chopper which interrupts a light beam between a small lamp and a phototransistor. The signal from the latter could be used to operate a high speed relay to effect the phase sensitive rectification.

(5) Detectors:-

No difficulty was experienced with the thermocouples employed. However, if measurements are to be made on the dark side of the moon, where temperatures down to more less -1[illegible] °C may prevail, they will almost certainly not be sensitive enough to detect small differences of temperature. In this case there appears to be no alternative but to employ a cooled detector, with its disadvantages of cryostats etc.

IV. PLANS FOR FURTHER OBSERVATIONS

(a) In the first place the measurements of emissivity should be repeated, as no values of this quantity exist, and all observers have up to now assumed that the Moon radiates in the infra-red as a black body.

(b) The observations on Proclus, Manilius, and Copernicus, should be extended with a view firstly to finding more anomalies of the same type, and correlating them with topographical features (if possible), and secondly by means of raster scans constructing isothermal contour maps of these craters and their surroundings.

(c) Observations of one of these anomalous craters throughout one complete lunation, to find the variation of the temperature and of the temperature differences with solar altitude. Observations just before the crater crosses the terminator into the sunlit hemisphere at waxing moon, and just after it crosses into the dark hemisphere at waning moon may give information as to the causes of the anomalies.

Manilius may be a suitable crater for this purpose, being near to the centre of the lunar disc, and receiving nearly maximum insolation at full moon.

(d) Planetary observations. During the observing trip none of the major planets were in a favourable position for observation. Given suitable conditions it should be possible to obtain temperature readings of Mars and Venus, and if the angular subtense of the planet at the time is sufficiently large several separate regions of the planet may be scanned and a crude thermal map prepared.

For more detailed planetary observations it would probably be necessary either to use more sensitive detectors, or a larger telescope, and construct a new instrument to fit onto the Cassegrain focus of the latter. The larger image of the planet at this focus will simplify any guiding problems.

REFERENCES

[1] Ring, J. Ph.D. thesis, Manchester 1957.

[2] Lissberger, P. Ph.D. thesis, Manchester 1957.

[3] Beer, R. Ph.D. thesis, Manchester 1960.

[4] Smith, S.D. J.O.S.A. *48*, 43, 1958.

[5] Pettit, E. & Nicholson, S.B. Ap.J. *71*, 102, 1930.

[6] Piddington, J.H. & Minnet, H.C. Austr. J. Sci. Res. *2*, 63, 1949.

[7] Sinton, W.M. J.O.S.A. *45*, 975. 1955.

[8] Shorthill, R.W., Borough, H.C., & Conley, J.M. P.A.S.P. *72*, 481, 1960.

[9] Sinton, W.M. Lowell Obs. Bull. No. 104. Vol.IV. No.16.

[10] Sinton, W.M. Lowell Obs. Bull. No. 108. Vol. V. No. 3.

Dept. of Astronomy AF 61(052)-~~524~~ 400
Univ. of Manchester TN-1
Manchester, Gt. Britain Special Projects

LUNAR INFRA-RED MEASUREMENTS

R. STERNBERG.

ABSTRACT: A radiometer was designed and constructed to make observations of the Moon in the atmospheric window 8 - 13μ. The primary aim was to determine the emissivity of the lunar surface by measuring the radiant flux.

Dept. of Astronomy AF 61(052)-~~524~~ 400
Univ. of Manchester TN-1
Manchester, Gt. Britain Special Projects

LUNAR INFRA-RED MEASUREMENTS

R. STERNBERG.

ABSTRACT: A radiometer was designed and constructed to make observations of the Moon in the atmospheric window 8 - 13μ. The primary aim was to determine the emissivity of the lunar surface by measuring the radiant flux.

Dept. of Astronomy AF 61(052)-~~524~~ 400
Univ. of Manchester TN-1
Manchester, Gt. Britain Special Projects

LUNAR INFRA-RED MEASUREMENTS

R. STERNBERG.

ABSTRACT: A radiometer was designed and constructed to make observations of the Moon in the atmospheric window 8 - 13μ. The primary aim was to determine the emissivity of the lunar surface by measuring the radiant flux.

Dept. of Astronomy AF 61(052)-~~524~~ 400
Univ. of Manchester TN-1
Manchester, Gt. Britain Special Projects

LUNAR INFRA-RED MEASUREMENTS

R. STERNBERG.

ABSTRACT: A radiometer was designed and constructed to make observations of the Moon in the atmospheric window 8 - 13μ. The primary aim was to determine the emissivity of the lunar surface by measuring the radiant flux.